

Title	A 105cm Fixed Frequency Cyclotron of Kyoto University
Author(s)	Kimura, Kiichi; Uemura, Yoshiaki; Sonoda, Masateru; Shimizu, Sakae; Yanabu, Takuji; Ishiwari, Ryutarō; Kokame, Jun; Katase, Akira; Kumabe, Isao; Yamashita, Sukeaki; Takekoshi, Hidekuni; Miyake, Kozo; Ikegami, Hidetsugu; Fujita, Hirokazu
Citation	Bulletin of the Institute for Chemical Research, Kyoto University (1962), 39(6): 368-406
Issue Date	1962-03-25
URL	<a href="http://hdl.handle.net/2433/75872">http://hdl.handle.net/2433/75872</a>
Right	
Type	Departmental Bulletin Paper
Textversion	publisher

# A 105cm Fixed Frequency Cyclotron of Kyoto University

Kiichi KIMURA, Yoshiaki UEMURA, Masateru SONODA,<sup>a</sup>  
Sakae SHIMIZU,<sup>b</sup> Takuji YANABU, Ryutarō ISHIWARI,  
Jun KOKAME, Akira KATASE,<sup>a</sup> Isao KUMABE,<sup>c</sup>  
Sukeaki YAMASHITA, Hidekuni TAKEKOSHI,<sup>d</sup>  
Kozo MIYAKE, Hidetsugu IKEGAMI<sup>e</sup> and  
Hirokazu FUJITA\*

(Kimura Laboratory)

*Received February 10, 1962*

A 105 cm fixed frequency cyclotron at the Institute for Chemical Research, Kyoto University is described.

The azimuthal asymmetry of the magnetic field of the cyclotron has been reduced up to 0.01 %, and the median plane of the dees and that of the magnetic field coincide each other within 1 mm. In order to drive the self-excited oscillator above the "multipactoring" threshold, the dees and the dee-stems are electrically insulated and biased with a negative voltage. Therefore, the dee-stems are terminated by electric capacitors.

This cyclotron has been operated for several years producing internal and external beams of 7.5 Mev protons, 15 Mev deuterons and 30 Mev alpha particles. These beams are now being used for various experiments on nuclear reactions and for producing radioisotopes.

## CONTENTS

1. Introduction .....	369
2. Specifications and Performances .....	371
3. Building and General Arrangement of the Equipments .....	371
4. Components of the Cyclotron .....	372
A. Magnet .....	372
B. Vacuum Envelope .....	376
C. Resonant Circuit and Oscillator .....	379
D. Ion Source .....	386
E. Deflection System .....	388
F. Vacuum System .....	391
G. Cooling System .....	394
H. Control System .....	396

<sup>a</sup> Now at Department of Nuclear Engineering, Faculty of Engineering, Kyushu University, Fukuoka.

<sup>b</sup> Now at Shimizu Laboratory, Institute for Chemical Research, Kyoto University, Kyoto.

<sup>c</sup> Department of Physics, Faculty of Science, Kyoto University, Kyoto.

<sup>d</sup> Now at Japan Atomic Energy Research Institute, Tokai-mura, Ibaraki-ken.

<sup>e</sup> Now at Institute for Nuclear Study, University of Tokyo, Tokyo.

\* 木村毅一, 植村吉明, 園田正明, 清水栄, 柳父琢治, 石割隆太郎, 小亀淳, 片瀬彬, 隈部功, 山下佐明, 竹腰秀邦, 三宅弘三, 池上栄胤, 富士田浩一

5. Performances .....	396
A. Minimum Dee-to-Dee Voltage .....	396
B. Initial Testing and Troubles .....	398
C. Some Improvements .....	402
6. Beam Focusing System and Scattering Chamber .....	403
7. Acknowledgements .....	405

## 1. INTRODUCTION

The Kyoto University had a plan to build a 100 cm cyclotron before the World War II, and this project was started under the direction of Professor Bunsaku Arakatsu,\* in 1942. During the difficult period of the War its construction progressed steadily. However, this cyclotron still under construction, two cyclotrons in the laboratory of Dr. Nishina in Tokyo and the other one in the Osaka University, both were in operation, were all destroyed and smashed away by the Occupation Forces by mistake immediately after the end of the War in November 1945. For few years after the War experimental researches on nuclear physics were also prohibited by an order of the Supreme Commander for the Allied Powers in Japan.

In May, 1951, the late Professor Ernest O. Lawrence of the University of California visited Japan. By many advices and encouragements which he generously extended to us of nuclear physicists and with the gradual rehabilitation in many fields of researches, the reconstruction of a cyclotron in the Kyoto University was proposed with general supports of the staff of the Kyoto University and the Ministry of Education. In 1952, the governmental budget for this project was granted by the Ministry of Education and a considerable amount of contribution was made. In response to this plan, Kyoto City kindly offered the use of the building which was used as a hydroelectric power plant in the past. The cyclotron was decided to build in this old building only about two kilometers far from the University main campus.

For this time, a 105 cm and 15 Mev ( $D^+$ ) fixed frequency cyclotron was newly designed. By the time when the design studies started, a few cyclotrons which have similar sizes had been constructed in MIT and other institutes. A number of useful review articles<sup>1,2,3,4</sup> on the theory and construction practices of cyclotrons were obtainable.

The design of this cyclotron is rather conservative, yet a few of new ideas are applied to it. The design had been finished by the fall of 1952, and then the parts were ordered to many companies for construction.

On November 16, 1955, an internal beam was first obtained at the radius of 40 cm. Within a short period, the internal beam reached the entrance of the deflection channel, and a deflected beam was observed on December 14, 1955.

During the next four years, constructions of shielding walls, ceilings, experimental rooms, and so on in the building had been performed. In the same time, intermittent testing of the cyclotron had been carried on. During this period, various kinds of radioisotopes were produced by the internal beams for many

\* Now, President of Konan University, Kobe.

research purposes.

In October, 1959, the beam focusing system was installed, and then a number of studies on nuclear reactions have been performed by using a scattering chamber. The main subjects of these studies so far are  $(p,p)$ ,<sup>5,6)</sup>  $(p,p')$ ,<sup>6,7)</sup>  $(d,\alpha)$ ,<sup>8,9)</sup>  $(p,\alpha)$ ,<sup>10,11)</sup>  $(\alpha,\alpha)$ ,<sup>12)</sup>  $(\alpha,\alpha')$  and  $(\alpha,p)$  reactions on various kinds of nuclei.

Continuous operation of this cyclotron for many hours is not available,

Table 1. Specifications and performances

1. Main Magnet <sup>a</sup>	
Total weight	79.8 tons Iron 71.3 tons Coils and Tanks 8.5 tons
Pole-base diameter	126 cm
Pole-tip diameter	105 cm
Pole-tip gap	13.5 cm
Magnetic induction at the gap	18,000 gauss, max
Distance between the septum and the center of the magnet	47.0 cm
Field fall-off at the septum	2.65 %, $n=0.36$
Coil	30 mm $\times$ 2.5 mm copper wire, total turns 2380, total resistance 3.45 $\Omega$ (60°C)
M-G set	100 hp, 75 kw dc
Current stability	$2 \times 10^{-4}$
Coil cooling oil	450 liters transformer oil
2. Vacuum System <sup>b</sup>	
Main diffusion pumps	40 cm diameter, speed 2,500 liters/sec $\times$ 2, 3-stages long nozzle type, fractionating oil
Fore diffusion pump	15 cm diameter, speed 80 liters/sec, one-stage long nozzle type, fractionating oil
Mechanical pump	Kinney type, speed 3,000 liters/min
3. Oscillator and resonant circuit <sup>c</sup>	
Resonant cavity	Coaxial double tube type, quarter-wave mode
Oscillator type	Grounded-grid self-excited, plate at high positive
Oscillator tubes	RCA 5671 $\times$ 2 (in parallel)
Dee	51 cm radius, 143° sector, Dee-to-earth capacity $\sim$ 350 pf
Power supply	6~12 kv, 10 amp, TEN <sup>d</sup> 7H57 $\times$ 6 or RCA 857 B, 6-phase single Y
Dee bias	About 500 v negative
Peak dee-to-dee voltage	About 90 kv
4. Ion source	
Type	Low voltage, hooded arc type
Filament	Hair pin type, 2 mm diameter wolfram wire heated by 6 v, 300 amp dc power supply
Arc power supply	300 v, 2 amp dc
Gas supplies	
Hydrogen and deuterium	Electrolytic cells of water and heavy water
Helium	AIR Co. high pressure vessel
Gas leak	Adjustable needle valves

5. Control			
Console	3 panels: Magnet current control and stabilizer ; vacuum pumps control, dee voltage and ion beam indicators, ion source and deflector controls ; oscillator control and compensator adjustment		
Q-magnet control panel	Current control and stabilizer, stability $10^{-3}$		
6. Performances <sup>e</sup>			
Particles	Energy (Mev)	Deflected beam ( $\mu\text{a}$ )	Beam at the scattering chamber <sup>f</sup> ( $\mu\text{a}$ )
Proton	7.5	90 <sup>g</sup>	0.1—0.3
Deuteron	15	90	0.1—0.3
Alpha particle	30	3	0.01

- The iron rods for the yoke and the upright were manufactured by Yahata Iron and Steel Co., Ltd., and they were machined by Sumitomo Metal Industries Ltd. The poles were manufactured by Sumitomo Metal Industries Ltd. The coil tanks and their cooling system were manufactured by Mitsubishi Electric Mfg. Co., Ltd., Itami Works.
- The oil diffusion pumps were manufactured by Kobe Steel Works, Ltd.
- The most parts of the resonant circuit were constructed by Kobe Steel Works, Ltd. The oscillator unit and its power supply were manufactured by Kobe Kogyo Corporation.
- This tube is made by Kobe Kogyo Corporation.
- Performances obtained by March, 1961.
- Beam intensity after passing through the 2 mm in diameter double slits, 36 cm apart.
- $\text{He}^+$  ion beam intensity.

but the weak points for this technical difficulty have been clarified and these parts are scheduled to be replaced in the very near future.

## 2. SPECIFICATIONS AND PERFORMANCES

Specifications and the performances are listed in Table 1. The deuteron and molecular hydrogen ion beams are strong enough to be utilized for nuclear research, while the alpha beam is somewhat weak. Some improvements in the ion source are still being carried on to increase the alpha-beam intensity.

## 3. BUILDING AND GENERAL ARRANGEMENT OF THE EQUIPMENTS

The building which houses the cyclotron was built as a hydroelectric power plant in the past, and had about 58 cm thick walls made of red bricks on the sides of the building, so that this made the construction of the radiation shielding easy.

Plan views of the main building are shown in Fig.1. The cyclotron and the main focusing system are arranged on the ground floor. In the room I, the cyclotron and a pair of quadrupole magnets are placed. The room II is used as an experimental room, and a scattering chamber, a sector magnet for beam analysis and a broad range magnetic spectrograph for detection of reaction particles are placed in this room. The room I is shielded by 110~160 cm thick concrete walls on the sides and a 70 cm thick concrete ceiling, while the room II is shielded by 80 cm

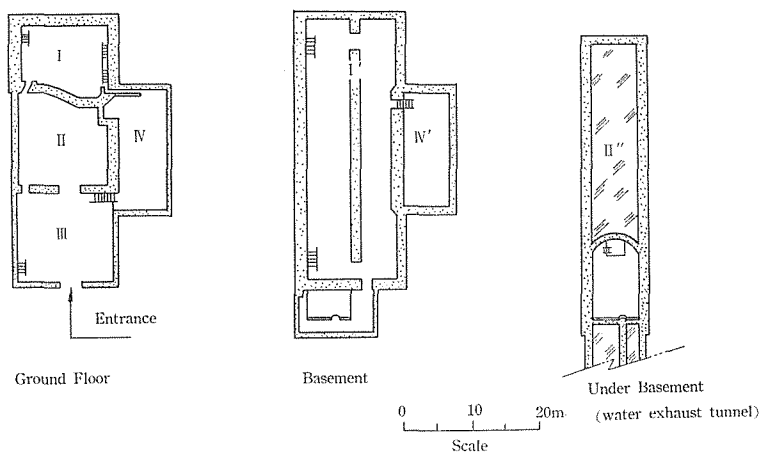


Fig. 1. Building.

thick concrete walls on three sides and a 50 cm thick concrete ceiling. The room IV having a higher floor than the ground floor is divided into two rooms, and they are used as control and counting rooms.

The cooling system consisting of three heat exchangers are installed in the room I' in the basement. Under the room I' there was a water exhaust tunnel of hydro-turbines. This tunnel serves now as a pool of cooling water supplied to heat exchangers. The dc generator for the cyclotron magnet and power transformers for power supply of the building are installed in the room IV'. A part of this room is used as a machine shop.

In Fig. 2, the general arrangement of the cyclotron and the beam focusing system is shown. The beam from the cyclotron is focused by a pair of quadrupole magnets, and then it is led through a beam duct into the scattering chamber in the experimental room. The beam analyzing magnet and the broad range magnetic spectrograph have been constructed and they will be fixed in place in the near future, for nuclear researches with higher energy resolution.

#### 4. COMPONENTS OF THE CYCLOTRON

##### A. Magnet

The magnetic circuit with the coil tanks in position is shown in Fig. 3. In order to accelerate deuterons up to 15 Mev, the diameter of these magnet poles requires the magnetic induction of 18 kilogauss. Therefore, some cares were taken in construction of the magnet to produce such a strong magnetic field in desirable shape.

The various pieces of the magnet are made of mild iron with low carbon and especially low manganese contents. The impurities of the iron used for the magnet are listed in Table 2. Each yoke and upright consist of three pieces and two pieces of rectangular iron rods, respectively. The permeability  $\mu$  of each piece was measured with various magnetic fields and is shown in Fig. 4. Therefore,

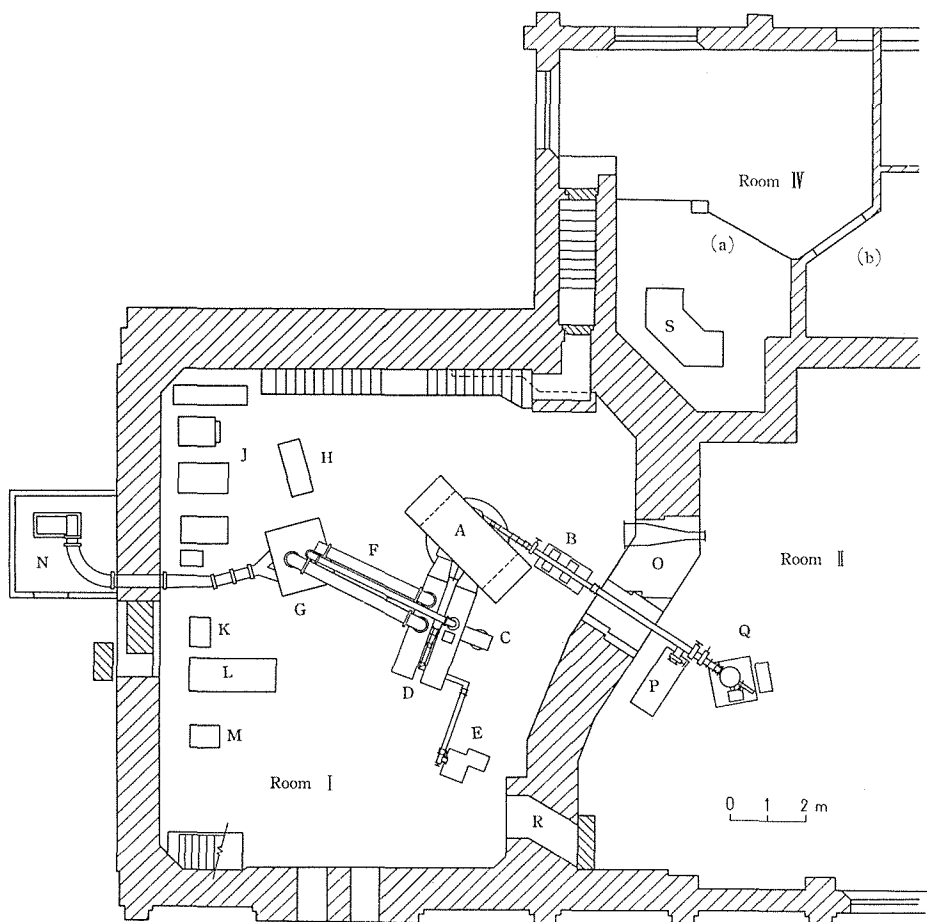


Fig. 2. General arrangement of the cyclotron and the beam focusing system.

- |  |   |
|--|---|
| R-I. Cyclotron room,                     | R-IV-a. Control room,                         |
| R-II. Experimental room,                 | R-IV-b. Counting room,                        |
| A. Cyclotron magnet,                     | L. Deflector high voltage power supply,       |
| B. Focusing magnet (Quadrupole magnets), | M. Ion source filament power supply,          |
| C. Main oil diffusion pump,              | N. Air intake for oscillator tube cooling,    |
| D. Dee-stem-tanks,                       | O. Water tank,                                |
| E. Mechanical pump,                      | P. Pumping system for the external beam duct, |
| F. Transmission lines,                   | Q. Scattering chamber,                        |
| G. Oscillator unit,                      | R. Passage,                                   |
| H. Oscillator control panel,             | S. Console.                                   |
| J. Oscillator power supply,              |   |
| K. Ion source arc power supply,          |   |

it was possible to combine these iron rods, so that each yoke and upright possess the similar permeability.

The tapered poles contain much less carbon than the yoke. These poles and

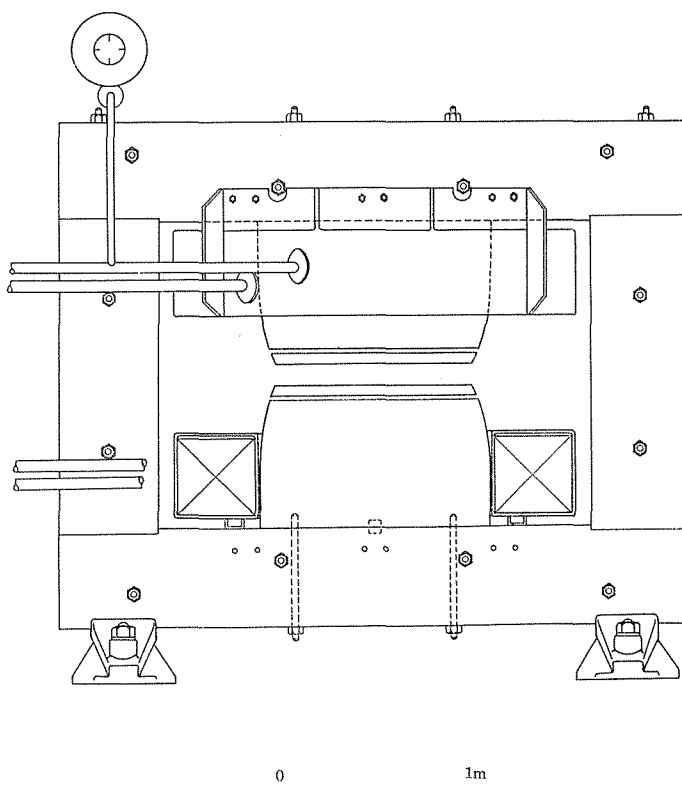


Fig. 3. Magnetic circuit with the coil tanks in position.

the pole-tips are formed into the shape suggested by Bethe\* to minimize the fringing flux. Furthermore, the parts of the coil tank walls which are facing to the pole or the other coil are made of non-magnetic stainless steel to avoid increasing of the flinging flux.

The pole-tips of 105 cm in diameter and 6 cm thick are used as lids of the dee-chamber and have solid ring shims (Rose-shims) of 20 mm wide and 7 mm high along their circumferences. The width of the Rose-shim is about twice of the calculated value using the formula given by Rose.<sup>13)</sup> Steel central shims are also provided and screwed down to the pole-tips.

Shimming gaps of 6 mm wide are left between the lids and the pole faces to correct deviations from the uniform field. The distance between the pole faces has been measured by a screw micrometer made of non-magnetic metal and found to be uniform within 0.03 mm when the magnet was excited.

The absolute magnetic field strength has been measured by the method of deuteron magnetic resonance, and the magnetization curve is shown in Fig. 5. This curve is linear up to 11 kilogauss with respect to ampere-turns.

The radial and azimuthal field variations for various excitations have been

\* The formula derived by Bethe is given in the paper by W.J. Henderson, L.D.P. King, J.R. Risser, H.J. Yearian and J.D. Howe, *J. Franklin Inst.* 226, 563 (1938)



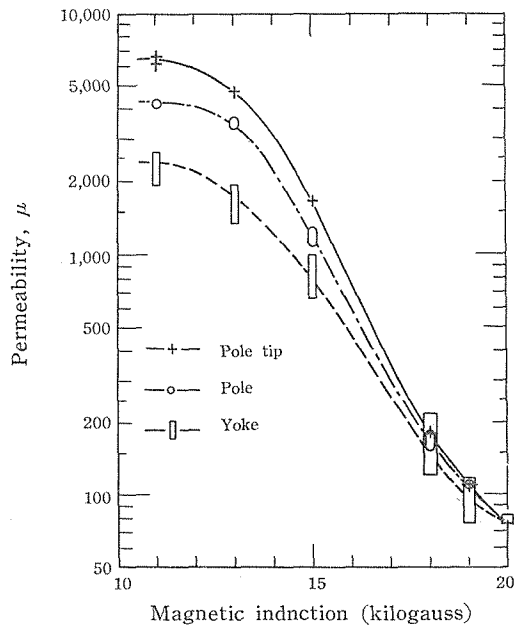


Fig. 4. Permeability of each iron piece of the magnet.

Table 2. Impurities of the iron used for the magnet.

Impurities Parts	C	Si	Mn	P	S	Cu	Cr	Al	Production process
Yoke	0.06 ~0.07	0.21 ~0.31	0.20 ~0.50	0.014 ~0.022	0.021 ~0.038	(0.16)	—	—	Open-hearth furnace
Pole	0.03 ~0.04	0.11 ~0.12	0.20 ~0.23	0.007 ~0.008	0.021 ~0.023	0.01 ~0.02	0.05	—	Arc furnace
Pole tip	0.05	0.17	0.27	0.005	0.014	0.16	0.04	0.27	Arc furnace

measured by an electronic fluxmetre of the type developed by Banks,\* and the results are shown in Figs. 6 and 7. As is shown in Figs. 7 and 8, the azimuthal asymmetry of the magnetic field has been reduced to be less than 0.01 % by inserting an adequate shimming plate made of a 0.35 cm thick silicon steel sheet in the lower shimming gap.

The median plane of the magnetic field has been measured for various radii by the method of a wire hoop\*\* and found to agree with the geometrical median plane within 0.2 mm inside the pole tips.

Each coil of the exciting coils consists of ten pancakes which are layers of 119 turns each, and sealed into the coil tank. Adequate cooling is provided by circulating transformer oil over the windings and subsequently through a heat exchanger cooled by water.

The power for the coils is supplied from a 400 volts dc generator\*\*\* driven

\* The details are described in Volume I of Reference 4.

\*\* The details are described in Volume III of Reference 4.

\*\*\* This generator is made by A.E.G., Germany, and offered from the electric power station of the Kyoto University.

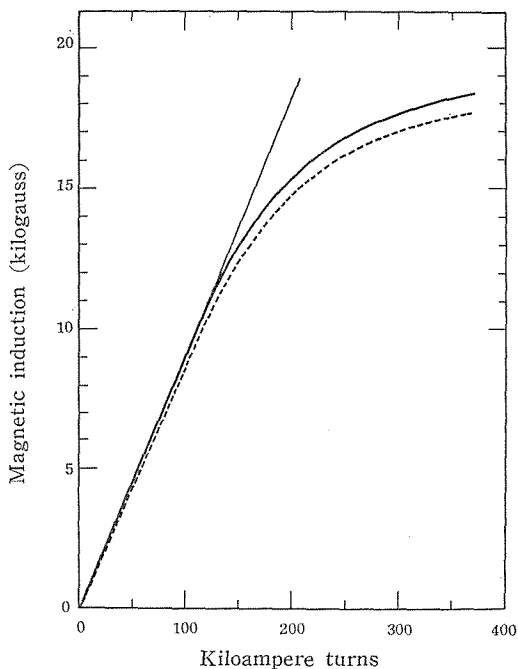


Fig. 5. Magnetization curve. The solid line shows the magnetization curve with a 12 mm shimming gap, and the dotted line shows that with a 1 mm shimming gap.

by an induction motor. The field of this generator is excited by a small generator of which field is excited by electron tubes to regulate the coil current. The regulator system is similar to that of the type developed by Danforth<sup>14)</sup> and is shown in Fig. 9 schematically. The reference voltage for this regulator is obtained from a precision potentiometer of which current is supplied from a 2 volts lead battery being charged by a 6 volts lead battery. The stability of the magnet current is 0.02 % for several hours.

### B. Vacuum Envelope

The vacuum envelope consists of two parts, the dee-chamber and two dee-stem-tanks made of copper pipes, which are seen in Fig. 10. The dee-chamber are made of 4 cm thick top and bottom brass plates with large circular holes for the pole tips which form the lids. The side walls are 3.2 cm thick brass plates and brazed by 53 % silver solder to form the dee-chamber structure. These brass plates used to construct the dee-chamber are non-magnetic and contain 70 % copper and 30 % zinc.

At the center of the large back opening (the dee-port) joining the dee-chamber to the dee-stem-tanks, a stanchion support is provided. On the side walls, four 11 cm diameter windows are provided to make it possible to inspect the internal structure. The pole-tips are positioned accurately by metal to metal contact and sealed by rubber gaskets of square cross section in the grooves

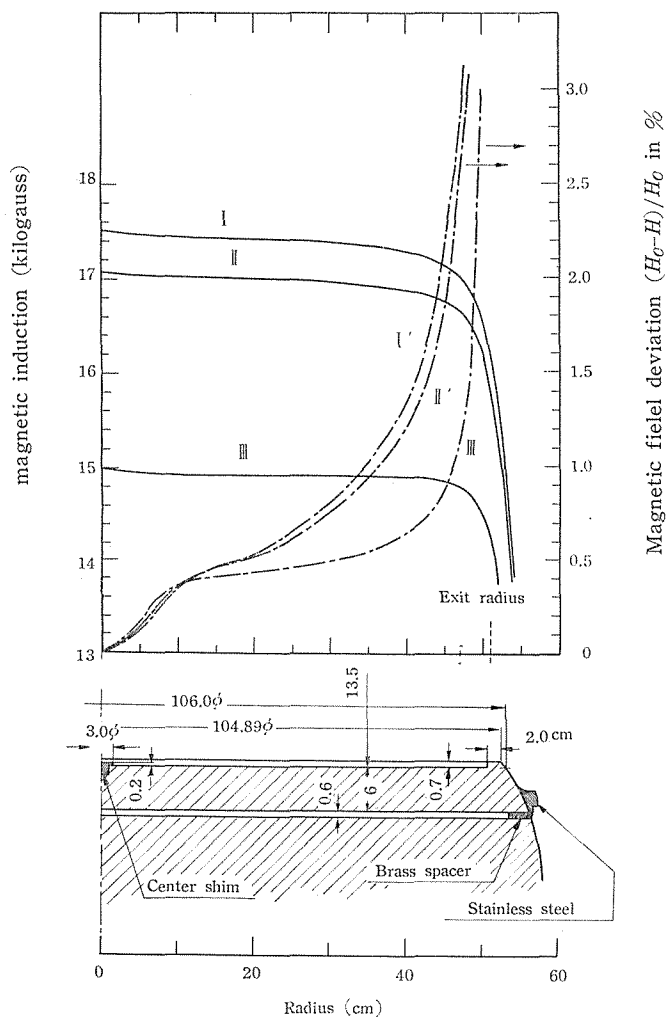


Fig. 6. Radial field distribution of the magnet and the cross-sectional drawing of the pole tip. Curves I, II and III show the radial dependence of the magnetic induction for currents of 138.0, 124.0 and 87.0 amperes, respectively. Curves I', II' and III' show the corresponding magnetic field deviation in percent.

between the pole-tips and the frames.

The dee-chamber is fixed tightly between the poles by inserting adequate brass spacers in the shimming gaps.

The distance between the pole tips under vacuum or with the strong cyclotron magnetic field was measured at eight positions just inside the Rose-shim, and their features are shown in Fig. 11. The results show that the pole tips are supported rigidly at the points A, B and C, since these points are closest to the side walls.

In order to provide better electric conductivity, the inner surfaces of the

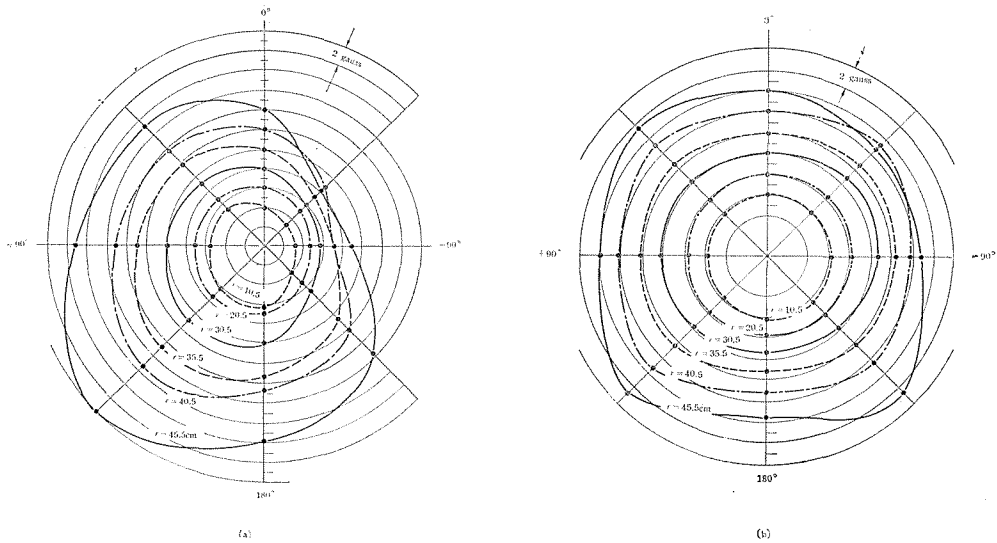


Fig. 7. Azimuthal field variation of the magnet. (a); without shimming, (b); with shimming. Concentric circles indicate the relative difference of the magnetic induction at the same radius. Therefore, for example, in (a), the magnetic induction at 180° and at the radius of 45.5 cm is 5.9 gauss lower than at 0° and  $r=45.5$  cm. The angular position with respect to the dee-chamber is shown in Fig. 8. In both cases, the magnet current was 135.35 amp.

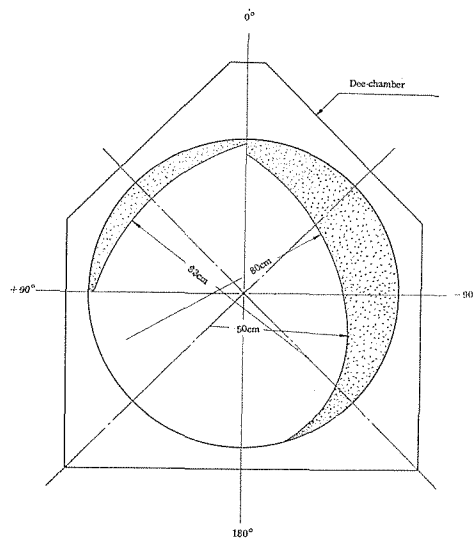


Fig. 8. Shape of the shimming plate. Two semilunar parts which are marked by dots indicate the shape of the shimming plates. The pentagonal flange indicates the dee-chamber.

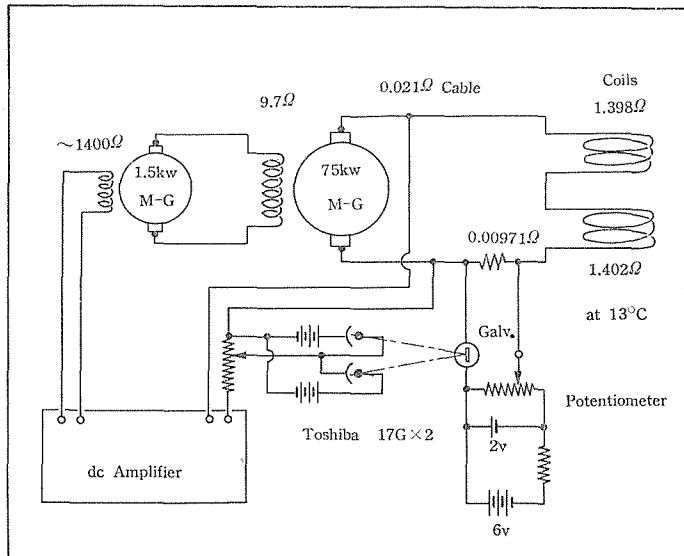


Fig. 9. Schematic diagram of the regulator system of the main magnet current.

pole-tips are covered with 2 mm thick copper liners with many 5 mm holes for quick evacuation of the volume between these sheets and the pole-tips.

The dee-stem-tanks are made of 8 mm thick and 60 cm in diameter copper pipes, and serve as the vacuum walls. The distance between the axes of these two tanks is 80 cm. The forward ends of these tanks are flattened into an oval section and connected to a common flange which joins to the dee-port of the dee-chamber.

The vacuum pumps are attached to the dee-stem-tanks as is shown in Fig. 10, and they evacuate the tanks through slits on the dee-stem-tank walls. These slits are made along the tank axis, so that they do not disturb the uniform rf current distribution on the inner surfaces of the dee-stem-tanks.

The dee-stem-tanks, the vacuum pumps and other attachments are all hung from a trolley on a girder. This trolley can be rolled back away from the magnet by the aid of a chain-drive mechanism with a 1/4 hp motor. On the other hand, the dee-chamber sits on rails with adjustable brackets which are affixed on the side wall of the lower coil tank, so that this arrangement permits to locate the chamber position accurately within the pole gap. These rails can be extended so as to withdraw the chamber from the pole gap to the other side of the magnet. The above mentioned structure greatly facilitates assembly or repairs of the dees and other internal structures, and the use of the trolley leaves enough space under the dee-stem-tanks for general assembly.

### C. Resonant Circuit and Oscillator

A couple of electrically shorted coaxial quarter-wave-lines with a dee as a capacity load across the end has been chosen as the resonant circuit. Furthermore, in

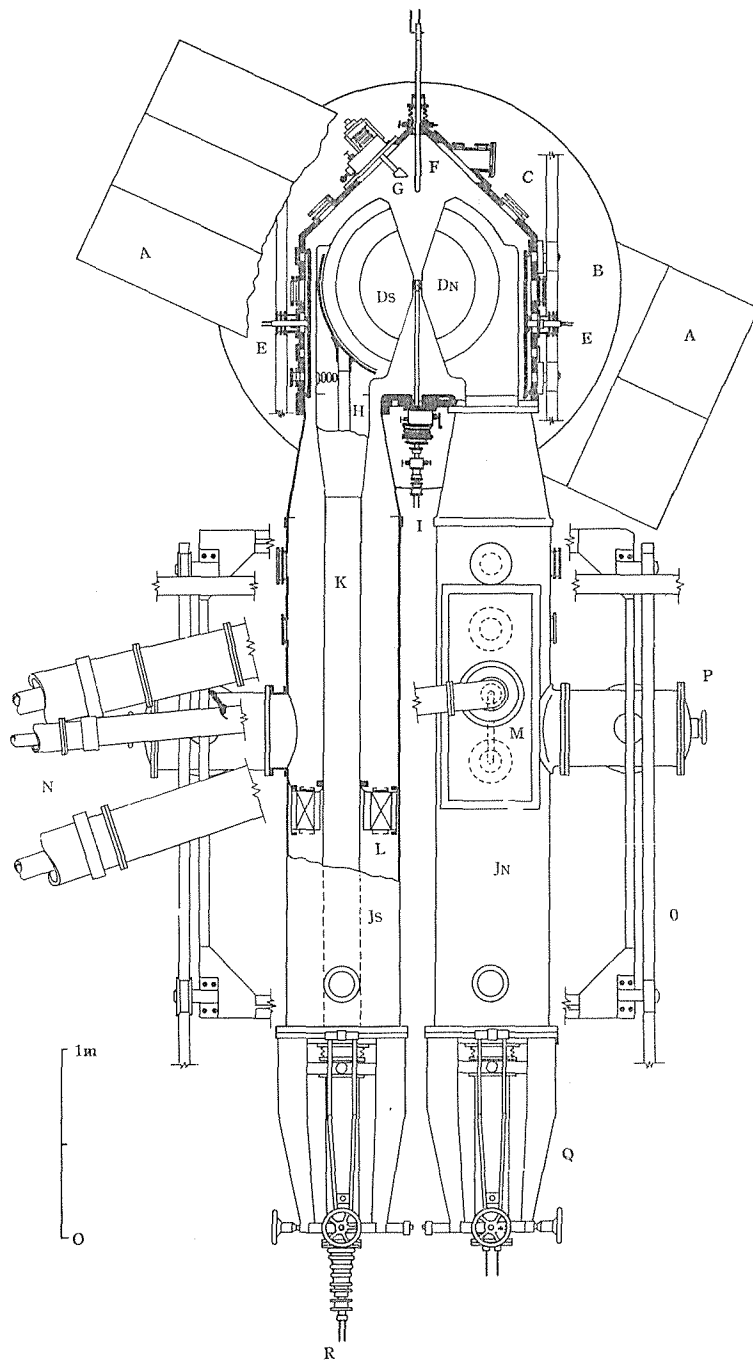


Fig. 10. Plan view of the cyclotron.

- |                             |                     |
|-----------------------------|---------------------|
| A. Cyclotron magnet,        | E. Compensator,     |
| B. Coil tank,               | F. Probe,           |
| C. Dee-chamber,             | G. Internal target, |
| D <sub>N</sub> . North dee, | H. Deflector,       |
| D <sub>S</sub> . South dee, | I. Ion source,      |

J<sub>N</sub>. North dee-stem-tank,  
 J<sub>S</sub>. South dee-stem-tank,  
 K. Dee-stem,  
 L. Short-circuiting capacitor,  
 M. Coupling box (north side),  
 N. Transmission lines,

O. Girder,  
 P. Main oil diffusion pump,  
 Q. Four-legged bracket supporting the  
 dee-stem,  
 R. Deflector-stem end.

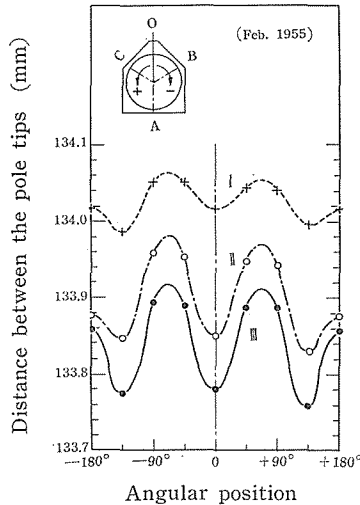


Fig. 11. Distance between the pole-tips. The distance was measured just inside the Rose-shim in Feb., 1955.

Curve I: 1 atm inside the dee-chamber

II: vacuum inside the dee-chamber

III: vacuum inside the dee-chamber and with the magnetic field on.

order to overcome the low-voltage electron loading phenomenon called “multipactoring”<sup>15,16)</sup> which plagues the self-excited oscillator, the quarter-wave-lines are terminated by electric capacitors so as to apply an adequate bias voltage. This resonant circuit and grounded-grid oscillator tubes are coupled together through transmission lines by coupling loops inside the dee-stem-tanks, and form a self-excited oscillator system.<sup>17)</sup> A schematic diagram of the whole circuit is shown in Fig. 12.

Since many electrical constants and characteristics of the resonant circuit seemed to be difficult to estimate by calculations, the full-size model of the whole resonant circuit was constructed from copper plates and iron frames prior to the final design of the oscillator system. By using this model and a small power oscillator, the electrical constants and characteristics of the resonant circuit of the cyclotron were estimated and useful knowledge on its many other properties was accumulated.

As is seen in Fig. 10, both dees are formed into the same shape to provide the same electric characteristics. They are “tapered off” to reduce the dee-to-earth capacity, so that the angle between the edges of dees is 37°. Furthermore, the height of the dee at the center part is 6.4 cm and tapered to 5.4 cm at the radius of 43 cm.

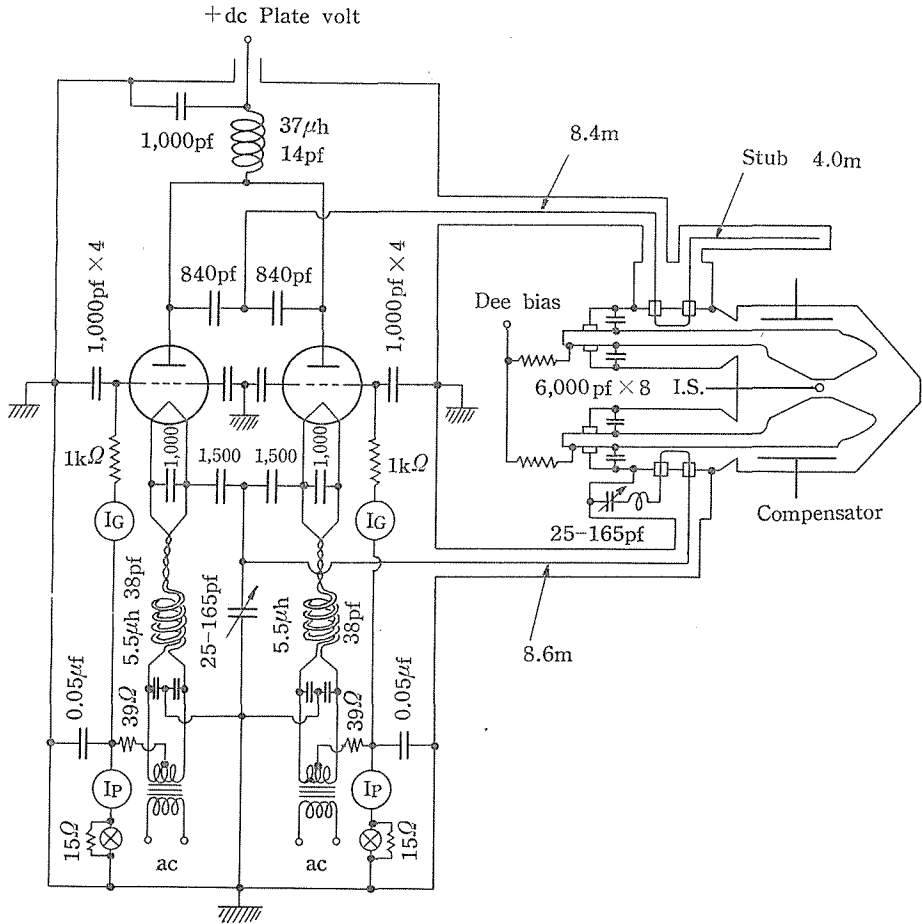


Fig. 12. Schematic diagram of the oscillator system.

The structure of the dee is shown in Fig. 13 in detail. Each dee consists of two dee-shells, "A", and their frame, "B", and then it is affixed to the end of the dee-stem. The dee-shells are manufactured from 2 mm thick copper plates having internal cooling lines which are soft-soldered to the inner surfaces of the dee-shells. The spacing of the cooling line is as short as 4.6 cm, so that it serves as a rib of the dee-shell. The cooling lines are made of 10 mm copper tubes which are flattened into an oval cross section of 6 mm high to increase the dee height available to the resonant beam. These dee-shells are screwed to the peripheral frame made of copper to form the desired shape, and are affixed to the extension rods of the dee-stem by screws.

Feelers of jaw type made of Cu-W sintered metal (30 % copper and 70 % wolfram) are attached to the upper and lower edges of both dees. This type of feeler should be less critical with respect to the positioning of the ion source than a vertical feeler, and sufficient resonant ion beams have been obtained with this feeler.



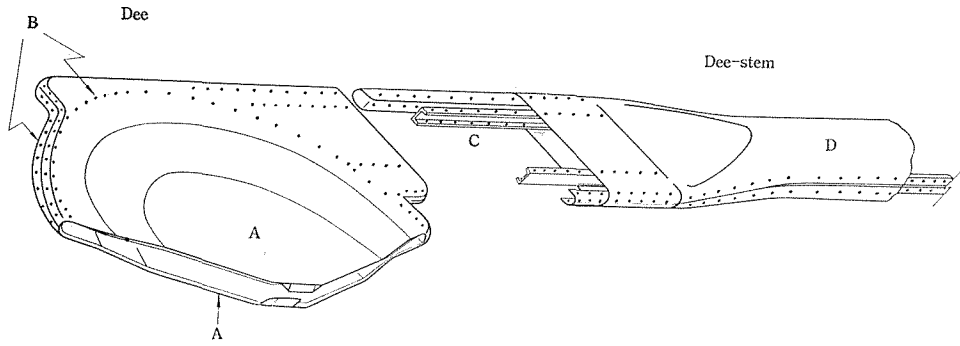


Fig. 13. Illustration of the connection between the dee and the dee-stem.  
 A. Dee-shells, B. Dee-frame,  
 C. Extension rods of the dee-stem, D. Dee-stem-shell.

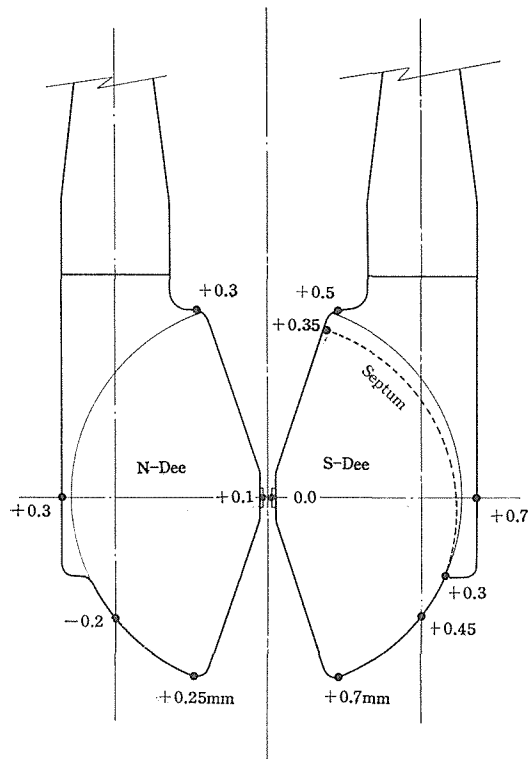


Fig. 14. Relative height of the dees with respect to the median plane.  
 The values seen beside the dots indicate the relative heights with respect to the geometrical median plane. These values were measured after the final setting of the dees, in May, 1960.

The dee-stem consists of a long steel pipe and copper shell which cover the steel pipe and provide better electric conductivity. The outer diameter of the dee-stem-shell is 20.3 cm and its thickness is 3 mm. This shell splits into two

parts longitudinally, so that the top and bottom halves can be separated to install cooling lines. These cooling lines consisting of 10 mm copper tubes are soft-soldered on the inner surface of the shell.

The steel pipe having a diameter of 15.5 cm and a length of 384 cm projects through a hole on the end lid of the stem tank, and is attached to an insulated four-legged bracket affixed to the lid. Screw adjustments on the bracket legs permit accurate positioning of the dees, and this adjusting mechanism allows to displace the end of the dees by 10 cm in the vertical and horizontal directions, by 2 cm along the axis and to rotate by 5.2 degrees around the stem axis.

The dee-stem-shell is fixed to this steel pipe by the aid of fingers and screws. The forward end of the steel pipe is kept about 14 cm away from the coil tanks. Therefore, the displacement of the dee position due to the cyclotron magnetic field is almost negligible; the dee was pressed down by only 0.4 mm and no horizontal displacement has been observed.

The position of the dee was set with great cares, so that the dee-median plane coincides with the magnetic median plane within 1 mm. The measured position after the adjustment is shown in Fig. 14.

Each dee-stem is terminated by a short-circuiting capacitor consisting of eight condensers which are installed in the space between the dee-stem and its tank. Each condenser<sup>18,19)</sup> with a capacity of 6000 pf consists of 1 mm thick aluminum plates spacing a gap of 1.5 mm. An adequate device with worm gears presses a number of 0.5 mm thick copper sheets from these unit condensers into electric contact with the dee-stem or the dee-stem-tank. The position of this termination

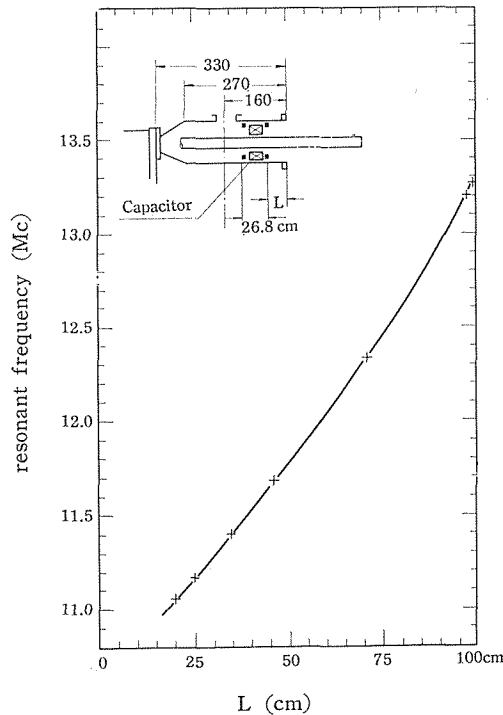


Fig. 15. Resonant frequency versus the position of the short-circuiting capacitor.

can be changed manually, but it is needed to break the cyclotron vacuum. The obtainable frequency range is from 11.0 to 13.0 Mc, as is shown in Fig. 15.

Before the assembly of the resonant circuit, a dc bias voltage necessary to stop the discharge inside the condenser under vacuum was measured by applying 12 Mc rf field to the condenser. This voltage is plotted in Fig. 16. The rf peak voltage across the short-circuiting capacitor at actual operation of the cyclotron was estimated to range between 400 and 650 volts. The pressure inside the cyclotron was expected to be lower than  $1 \times 10^{-4}$  mm Hg. Therefore, the voltage of 600 volts is sufficient for the dee-stem bias. At the same time the rf power dissipated in this condenser was estimated by measuring the power which was carried off from the condenser by cooling water. This power loss is shown in Fig. 17.

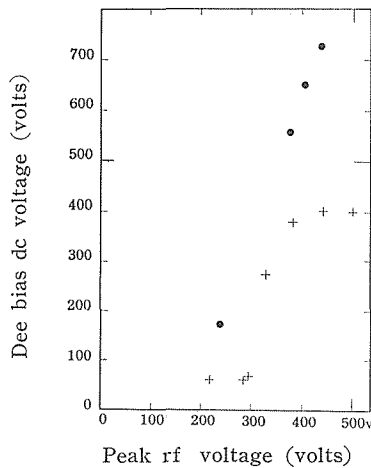


Fig. 16. Voltage necessary to stop the discharge inside the condenser. The crosses and the solid circles indicate the measured values at the pressures of  $1 \times 10^{-4}$  mm Hg and  $1.6 \times 10^{-4}$  mm Hg, respectively.

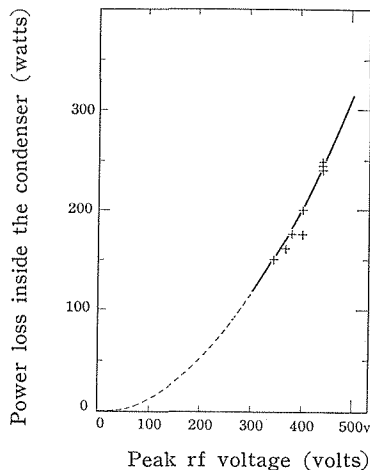


Fig. 17. rf power loss inside the condenser versus the applied peak rf voltage.

Table 3. Resonant frequency and the Q-value of the resonant circuit.

Oscillation modes	Measured resonant frequency in Mc*		Q
Single dee (other dee grounded)	N-Dee	13.2187	3,900
	S-Dee	13.2180	4,100
Parallel	13.2642		4,500
Push pull (1 atm inside the dee-chamber)	13.1721		4,400
Push pull (vacuum inside the dee-chamber)	13.1460		—

\* The compensator can shift the resonant frequency by 190 kc.

The resonant frequency of the resonant circuit and its width were measured using a small power rf oscillator. The values of the resonant frequency and the Q-value of the resonant circuit are listed in Table 3 for various modes of oscillation.<sup>17,20)</sup> Using the results listed in this table, the dee-to-dee capacity is estimated to be about 2.5 pf.

The oscillator unit shown in Fig. 12 is placed beside the cyclotron. Two RCA 5617 tubes are used in parallel and coaxial transmission lines lead from the plate and the cathode of the tubes to the coupling loops inside the dee-stem-tanks. The dimension of coaxial lines is; 30 cm outer shell diameter and 10 cm inner line diameter for the plate lines, and 15 cm o.d. and 5 cm i.d. for the cathode lines. The outer shell and the internal line are insulated by polystyrene disks.

The grid bias of the oscillator tube under oscillation is provided by an 1 k $\Omega$  resistor. On the other hand, when the oscillator stops oscillating due to discharges inside the tanks, the cathode is biased with a 39  $\Omega$  resistor to limit the excessively high plate current.

Power for the oscillator is supplied from a rectifier unit of six-phase single Y employing six RCA 857B or TEN 7H57 mercury vapor tubes. An output filter circuit consisting of a 0.5 henry choke and an 1  $\mu$ f capacitor. This power supply controls the oscillator plate voltage at any point in the voltage range between 6 kv and 12 kv by means of an induction regulator.

#### D. Ion Source

The ion source used is essentially a type of low-voltage gaseous discharge within a small metallic cavity.<sup>21)</sup> The discharge is maintained by electrons emitted from a dc heated filament. The whole assembly can be extracted through an air lock for repair, and the wolfram filament also can be extracted separately through an extra air lock for frequent replacement without extracting the whole assembly.

The initial design of the ion source was quite simple and is shown in Fig. 18. A few improvements have been made to increase the stability of cyclotron operation and the resonant ion beam. In March, 1958, a small insulated anode called "repeller" was installed at the top of the discharge cavity. However, when the power of gaseous discharge exceeded 250 watts, this anode was heated

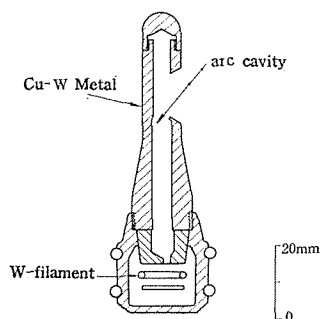


Fig. 18. Initial design of the ion source.

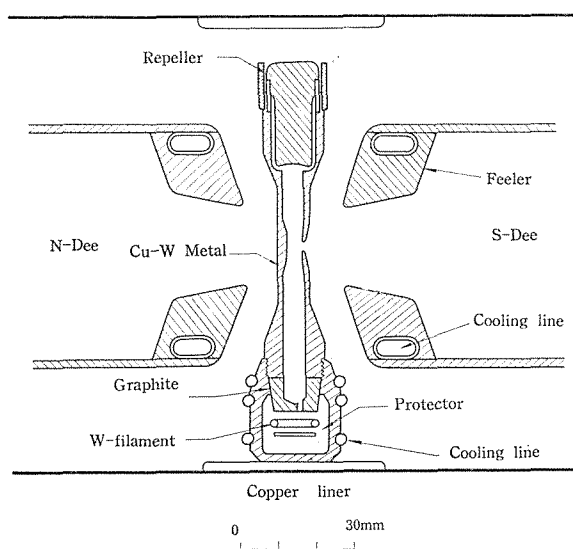


Fig. 19. Present ion source in place.

white hot, and then it emitted electrons which plagued the cyclotron operation. Therefore, in February, 1960, the repeller was replaced with new one having an increased surface area of  $12 \text{ cm}^2$  which provided enough thermal radiation, and the quartz insulator was shielded by a copper cap. The present ion source is shown in Fig. 19.

The filament used is a 2 mm diameter wolfram wire of hairpin type, and heated by dc from a selenium rectifier. The dc on the filament is about 200 amp and the discharge current varies from 0.5 to 1 amp at usual operation. A 0.5 mm thick tantalum plate placed under the filament protects the filament from ion bombardment from the bottom of the arc chamber. This arrangement lengthens the life time of the filament up to 300 hours which is about twice of that without the tantalum plate. After a few hundreds hour operation, usually the part of the filament right under the arc canal is consumed noticeably. Therefore, the characteristics of the filament, in particular its resistance, have changed during operation and these features are shown in Fig. 20.

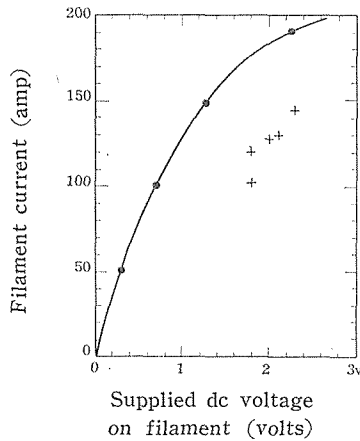


Fig. 20. Relation between the dc voltage and dc current of the ion source filament. The solid line shows a typical relation for a fresh filament. This curve was measured by loading the arc current of 0.9 amp with hydrogen. The cross indicates the relation for an old filament just before the break-down. The filament current and its voltage are about 190 amp and 1.8 v, respectively, under the normal operation.

A 2 mm diameter tantalum filament was also tested. However, this filament was deformed by the cyclotron magnetic field after 18 hour operation with the filament current from 160 to 180 amp.

The inner surface of the arc chamber was covered with a thin film of wolfram due to evaporation of the filament after several hundreds hour operation. This film caused sometimes the dead short between the filament and the arc chamber, so that it is necessary to clean up the arc chamber regularly.

Hydrogen or deuterium gas for the ion source is supplied from an electrolytic cell of light water or heavy water, respectively, and the helium gas used is supplied from a high pressure vessel. These gases are desiccated by the combination of silica gel and  $P_2O_5$  towers. The gas supply for the ion source is controlled by means of needle valves, one each for hydrogen, deuterium and helium.

Typical characteristics of the ion source are shown in Fig. 21, though the obtainable deflected beam of the cyclotron depends on various conditions.

### E. Deflection System

The resonant ion beam is extracted by an electrostatic field between the internal deflector and the septum. The distances from the center of the magnet to the entrance and exit of the septum are 47.0 and 51.0 cm, respectively. The value of  $n^*$  at the entrance is 0.36. The deflection channel starts at the point 3 cm inside from the dee edge and subtends 85 degrees in angle. This deflection channel is installed inside the dee structure and both dees have the exactly same shape.

\*  $n = -\frac{r}{H} \frac{dH}{dr}$ , where  $H$  denotes the magnetic inductance at the radius  $r$ .

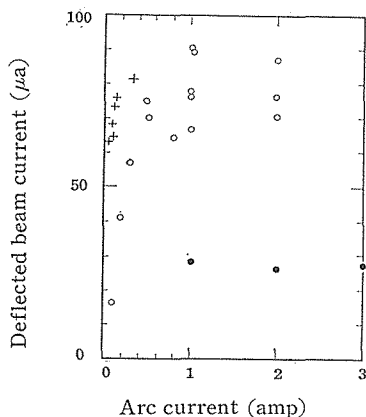


Fig. 21. Relation between the arc current of the ion source and the deflected beam.

Solid circle : 50 v arc voltage,

Open circle : 100 v arc voltage,

Cross : 100 v arc voltage, after a few day operation.

These values were measured under the other cyclotron condition as same as possible.

The foremost part of the septum is made of a 210 mm by 32 mm and 0.6 mm thick wolfram plate and fixed to a copper frame with a water cooling line and the rest of it is made of a copper plate. The deflector is also made of a copper plate and cooled by water.

The deflection system must fulfil certain requirements so as to extract the ion beam into the desired direction with the available high voltage supply. The fraction of the total resonant ions in the emergent beam should become greater as a deflection gap becomes wider, while a higher deflection voltage will be required. The maximum radial expansion<sup>23)</sup> between successive ion paths was estimated to be 7.8 mm at the radius of 47 cm for 15 Mev deuterons with a peak voltage of 150 kv. Taking into account all the requirements, the width of the deflection channel at the entrance was chosen to be 7.0 mm.

The ratio of the strengths of the electric and magnetic fields in the deflection channel has been chosen to be constant, since this type of field is considered to extract ions with relatively high efficiency and small angular divergence. The numerical and graphical calculations<sup>23)</sup> of the ion path have been performed under various conditions to determine the geometry of the deflection channel.

The intensity of the resonant beam before and after passing through the deflector has been measured by a sliding probe along the diametrical line between the dees. The results are plotted in Fig. 22. It is shown that the efficiency of ion extraction of the deflection system described is about 40 %. The deflected beam current versus the high voltage across the deflection channel is also shown in Fig. 23.

When the deflected ion current exceeds about 90  $\mu\text{a}$ , the discharge across the deflection channel started. This discharge might be due to the septum heated by ion bombardment, since after a few week operation the edge of the wolfram

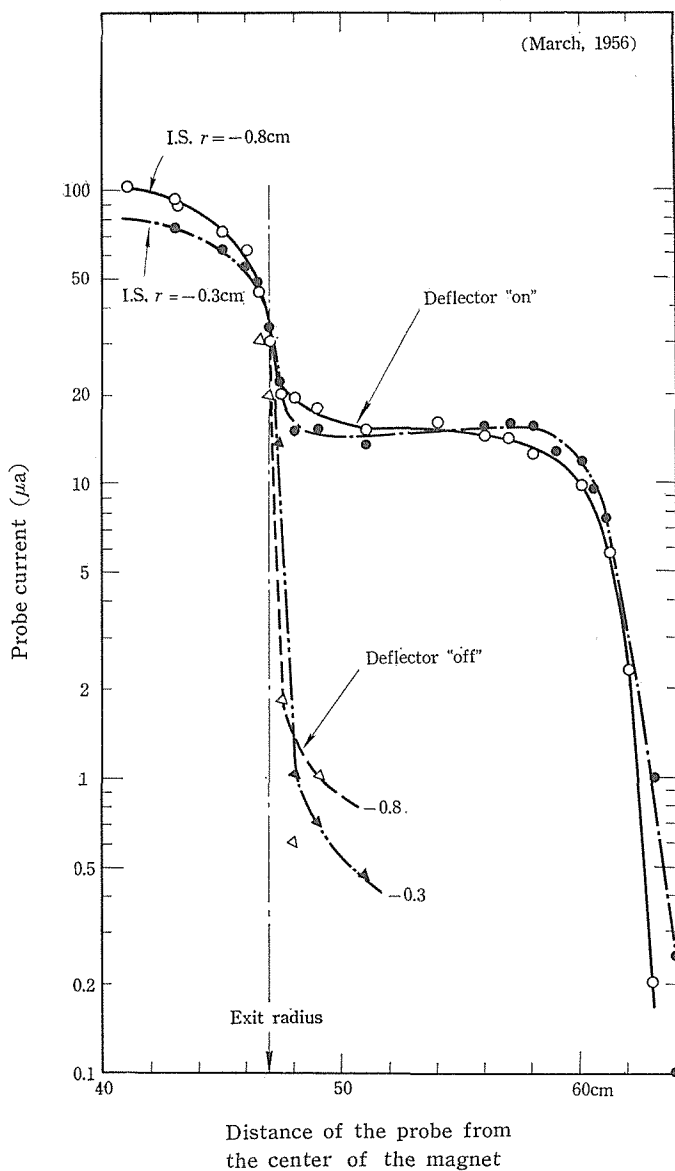


Fig. 22. Probe current with the deflector voltage of 36 kv and the peak dee-to-dee voltage of 115.5 kv.

Open circle : ion source at  $r = -0.8$  cm and deflector "on",  
 Open triangle : the same conditions with deflector "off",  
 Solid circle : ion source at  $r = -0.3$  cm and deflector "on",  
 Solid triangle : the same conditions with deflector "off".  $r = -0.8$  cm means that the ion source is drawn back by 0.8 cm from the center of the magnet toward the dee-stem-tanks.

plate at the entrance was melted. Therefore, the available deflected ion beam intensity seems to be less than  $90 \mu\text{A}$ .

The high voltage for the deflector is supplied from a conventional single



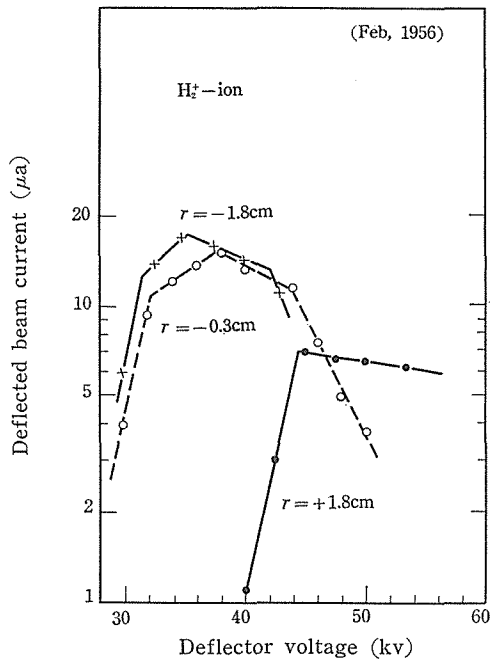


Fig. 23. Deflected beam current versus the ion source position.

Open circle : ion source at  $r = -0.3$  cm,

Cross : ion source at  $r = -1.8$  cm,

Solid circle : ion source at  $r = +1.8$  cm.

$r = -0.3$  cm means that the ion source is drawn back by 0.3 cm from the center of the magnet toward the dee-stem-tanks.

phase rectifier with a  $0.02 \mu\text{f}$  filter capacitor. A  $7 \text{ k}\Omega$ , 120 watts resistor is inserted between the deflector and the high voltage supply. This prevents heavy discharge from the deflector, which caused serious damages to the water cooling line of the deflector.

#### F. Vacuum System

A schematic diagram of the vacuum system is shown in Fig. 24 together with the conductance of vacuum tubing. The volume  $V$  of the vacuum envelope is  $2.37 \times 10^3$  liters and the area of its internal surface in contact with vacuum is  $7.2 \times 10^5 \text{ cm}^2$ . In order to obtain the reasonably high vacuum and the short pumping down time, the pumping speed  $S$  of the vacuum system should be as fast as  $2 \sim 3 \times 10^3$  liters/sec or faster.

However, at the time when the cyclotron was designed, any commercial pump with such high pumping speed was not available. Therefore, the 40 cm oil diffusion pump was designed, which has three stages of long nozzle type and fractionates oil. This pump has the pumping speed of 2500 liters/sec. Two identical pumps of this type were provided, and they evacuate the vacuum envelope in parallel through slits on both dee-stem-tanks. The pumping down time of this vacuum system is about 15 minutes, from  $1 \sim 2 \times 10^{-2} \text{ mm Hg}$  to  $4 \sim 6 \times 10^{-6} \text{ mm Hg}$ . However,

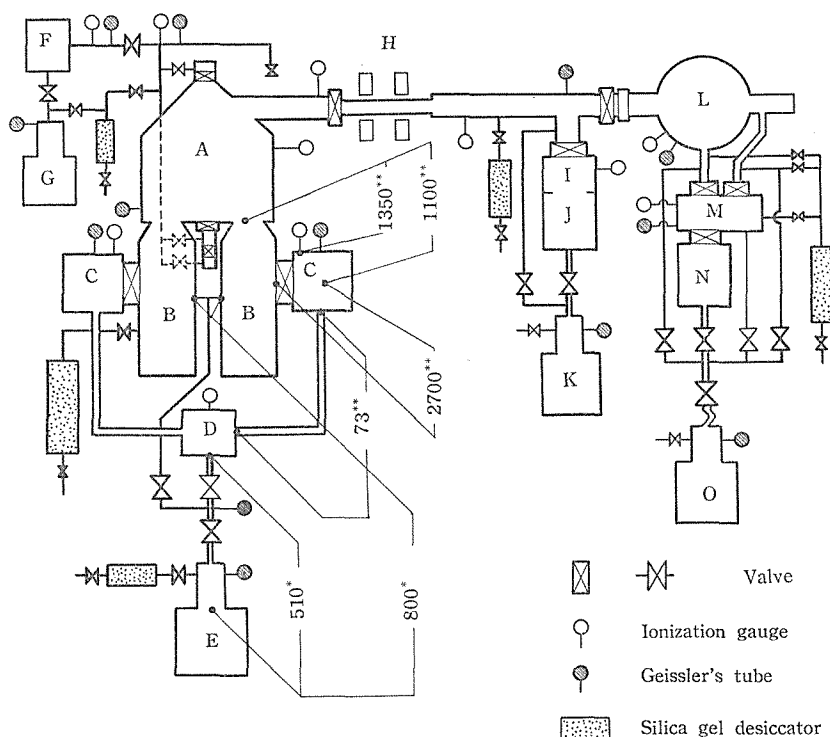


Fig. 24. Schematic diagram of the vacuum system.

- |                                     |                                    |
|-------------------------------------|------------------------------------|
| A. Dee-chamber,                     | I. Liquid-air trap,                |
| B. Dee-stem-tank,                   | J. 17.5 cm oil diffusion pump,     |
| C. 40 cm oil diffusion pump,        | K. 650 liters/min mechanical pump, |
| D. 15 cm oil diffusion pump,        | L. Scattering chamber,             |
| E. 3000 liters/min mechanical pump, | M. Liquid-air trap,                |
| F. 7.5 cm oil diffusion pump,       | N. 16 cm oil diffusion pump,       |
| G. 200 liters/min mechanical pump,  | O. 800 liters/min mechanical pump. |
| H. Pair of quadrupole magnets,      |                                    |

The numbers in this figure show conductance of the piping, and their units are ; \*=liters/min, \*\*=liters/sec.

these two main diffusion pumps have a quite large heat capacity, so that it takes about one hour and 20 minutes to warm up. The pumping down feature is shown in Fig. 25.

A careful leak hunting was performed for every parts used in the vacuum envelope before the assembling of the cyclotron. After the leak of each parts was found to be negligible by using an ionization gauge and propane gas as probe gas, the degassing rate  $Q_0$  was measured by the method of pressure rise. Although thus measured  $Q_0$  should contain some contributions from small leaks which are negligible, these are considered to be very close to the true values and listed in Table 4.

Most of the inner surfaces of the vacuum envelope are the surfaces of copper and aluminum, so that the average degassing rate  $Q_0$  is expected to be  $2 \times 10^{-9}$  mm Hg liters  $\text{cm}^{-2}$   $\text{sec}^{-1}$ . Therefore, the total degassing rate  $Q_T$  over the vacuum

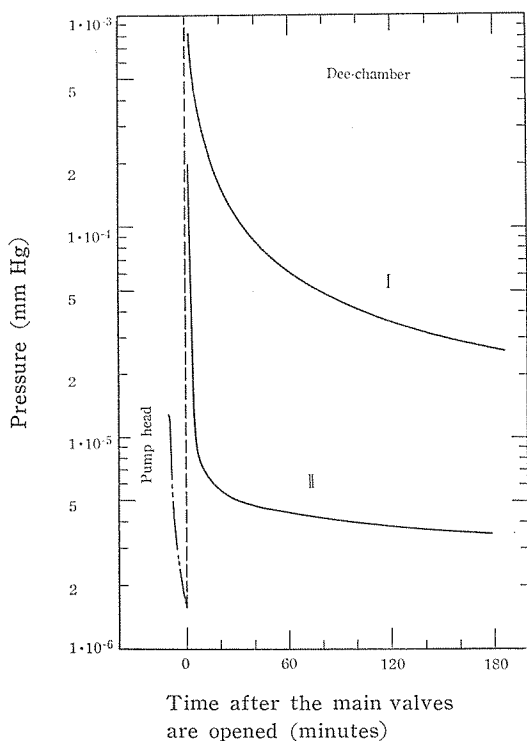


Fig. 25. Pumping down time. The curve I shows the behavior of the pressure inside the dee-chamber for the first evacuation, and the curve II shows that of the second or third evacuation.

Table 4. The measured degassing rate  $Q_0$  of the various surfaces of the parts used for the vacuum envelope.

Surface materials and conditions	$Q_0$ ( $\frac{\text{mm Hg}}{\text{sec cm}^2}$ )	Measured pressure (mm Hg)
Steel (rough surface)	$2.2 \times 10^{-8}$	$1 \times 10^{-4}$
Steel (baked surface)	$7.3 \times 10^{-9}$	$1-2 \times 10^{-4}$
Steel (machined surface)	$5.4 \times 10^{-9}$	$4-6 \times 10^{-5}$
Phosphor bronze (rolled)	$6.0 \times 10^{-9}$	$2-3 \times 10^{-5}$
Brass (rolled)	$7.6 \times 10^{-10}$	$2 \times 10^{-5}$
Copper (polished)	$1.9 \times 10^{-9}$	$3.2 \times 10^{-6}$

envelope should be  $1.4 \times 10^{-3}$  mm Hg liters/sec.

After the whole assembling of the cyclotron vacuum system, the extensive leak hunting aimed to reduce  $Q_T$  down to this expected value had been carried out. As was mentioned, the time constant of the cyclotron vacuum system,  $V/S$ , is about 1 sec. Thus, it made the leak hunting very easy. The leak has been found by evacuating the whole system by one of 40 cm pumps with an ionization gauge at the top of the pump and using propane gas as probe gas. For large leaks, the Geissler's tube and propane gas method was employed.

**G. Cooling System**

The cooling system of the cyclotron is divided into four sections which are listed in Table 5 together with the values of power dissipated, the cooling materials and the methods of cooling.

Pure water obtained by the method of ion exchange is used as the cooling material for the dees and dee-stems which must be insulated electrically. The use of pure water protects cooling lines from erosion by electrolysis and also deposit of fur. The resistance between the dee and earth can be raised as high as 90 MΩ by purification of water. However, no trouble has been found even when this resistance became as low as 0.3 MΩ after long-term operation. Therefore, with respect to electric insulation, it is found to be unnecessary to use pure water.

A schematic diagram of the cooling system is shown in Fig. 26. Three heat exchangers and their centrifugal pumps for the sections I, III and IV are installed

Table 5. Cooling system

Section	Parts	Power dissipated	Cooling materials	Circulating rate and the power of the cooling system
I. Cyclotron magnet	Coils	65 kw	Transformer oil	Heat exchanger (16 m <sup>2</sup> ), Primary water ; 410 liters/min, 3 hp, oil ; 400 liters/min, 2hp.
II. Oscillator unit	Oscillator tubes, (RCA 5671)	25×2 kw	Forced air	Air ; 102 m <sup>3</sup> /min, 7.5 hp.
	Rectifiers (RCA 857B)	—	Forced air	Air ; 100 w moter.
III. Resonant circuit and the deflector	Dees, Dee-chamber, Dee-stems, Dee-stem-tanks, Capacitors, Deflector, Septum, Coupling loops,	8×2 kw 16 kw 12×2 kw 4×2 kw 2×2 kw 7.5 kw 7.5 kw 3 kw	Pure water	Heat exchanger (9.7 m <sup>2</sup> ), Primary water ; 150 liters/min, 2 hp, Pure water ; 250 liters/min, 2 hp.
	Transmission lines	4 kw		Air
IV. Vacuum pumps and the ion source	40 cm pumps, 15 cm pumps, Auxiliary pumps,	4×2 kw 2.5 kw 0.7 kw	Pure water	Heat exchanger (9.7 m <sup>2</sup> ), Primary water ; 150 liters/min, 2 hp, Pure water ; 250 liters/min, 2 hp.
	Ion source,	1.3 kw		(pressurized)
	Internal target,	15 kw	(pressurized)	1 hp gear pump ; 8-10 kg/cm <sup>2</sup> .
	Mechanical pump	3 kw	City water	

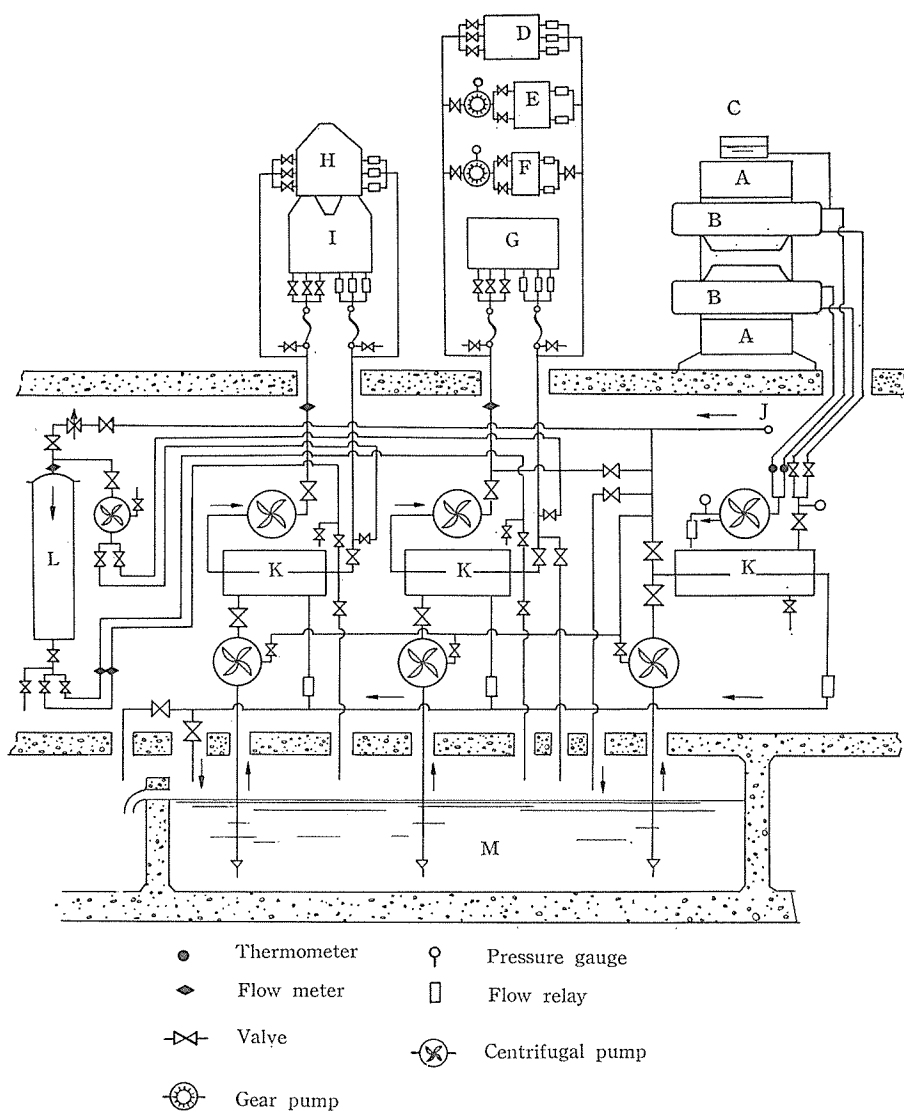


Fig. 26. Schematic diagram of the cooling system.

- |                         |                               |
|-------------------------|-------------------------------|
| A. Cyclotron magnet,    | H. Dee-chamber,               |
| B. Coil tank,           | I. Dee-stem-tanks,            |
| C. Oil level indicator, | J. City water intake,         |
| D. Auxiliary pumps,     | K. Heat exchangers,           |
| E. Internal target,     | L. Ion-exchanger resin tower, |
| F. Ion source,          | M. Pool.                      |
| G. Vacuum pumps,        |                               |

in the room I' under the cyclotron room. The pipes between these heat exchangers and the cyclotron consist of hard vinyl tubes for the sections III and IV, and iron is perfectly avoided. The cooling lines for the ion source and the internal target are made of thin copper pipes, so that these lines are needed to supply water by the aid of gear pumps made of stainless steel.

These heat exchangers use the water circulating from the pool under the room I. The volume of this pool is about 400 m<sup>3</sup>, and the temperature rise of the pool water after 24 hours continuous operation is found to be about 5.5°C.

During the initial testing of the cyclotron, it was found that the stray rf field beyond the dee-stem termination destroyed the vacuum seal of cooling lines on the end lids of the dee-stem-tank and caused vacuum leak. Therefore, the cooling pipes from the dees, the dee-stems and the termination capacitor are grounded by 1000 pf ceramic capacitors as by path, outside the vacuum envelope at their outlet points.

#### H. Control System

The control system of the cyclotron has been designed to make it possible to control the equipments either at the console or at the localized control panels which are located close to each equipment. Therefore, enough interlocks and switches are provided, whenever required, for safety of equipments. In addition to these interlocks, alarms and signal lights on the console panel or each localized control panel indicate defects or states of operation.

The console is placed in the room IV adjacent to the cyclotron room, but this room has about 3.4 m higher floor level than the cyclotron room. The shielding wall between the control and cyclotron rooms is made of ordinary concrete of 155 cm thick. The neutron flux in the control room is about  $2 \times 10^{-2}$  neutrons cm<sup>-2</sup> sec<sup>-1</sup> when the internal deuteron beam of 100  $\mu$ a and 15 Mev bombarded a copper target.

The console has three panel faces where a number of meters, signal lights, switches and handles for regulation are mounted. Some electronic circuits are mounted in this console, and they are the main magnet current stabilizer, the ion source arc current stabilizer and the vacuum gauge control.

The following meters and indicators were installed in the control room; a frequency meter, a phase indicator for rf oscillation of the resonant circuit, a rate meter for gamma-radiation in the cyclotron room and so on. These equipments are mounted on suitable racks beside the console.

All electrical and electro-mechanical units can be turned on and off and can be controlled at the console, though the mechanical valves such as the vacuum valves and the needle valves for gas supply of the ion source can not be controlled from the console.

### 5. PERFORMANCE

#### A. Minimum Dee-to-Dee Voltage

Before the initial testing of the cyclotron, the minimum dee-to-dee rf voltage necessary to obtain the resonant ion beam through the deflection channel was estimated. For this estimation, one must know the behavior of phase shift of an ion while it is accelerated from the ion source to the entrance of the deflector.

---

\* This fast neutron flux was measured by a "Nemo" neutron counter.

The phase shift  $\theta$  of the ion is given as follows,<sup>24,25)</sup>

$$\sin \theta = \int (F_1 - F_2) dE,$$

$$\text{with } F_1 = \frac{\pi}{2eV_o} \left( \frac{E_{res}}{Mc^2} + \frac{H_o - H_{res}}{H_o} \right), \quad F_2 = \frac{\pi}{2eV_o} \left( \frac{E}{Mc^2} + \frac{H_o - H}{H_o} \right),$$

where  $\theta$  denotes the phase shift,  $V_o$  is the accelerating peak voltage,  $E$  is the energy of the ion,  $H_o$  is the magnetic field strength at the center of magnet,  $H$  is the magnetic field strength at the position where the ion has the energy  $E$ ,  $E_{res}$  is the energy of the ion of which angular velocity coincides with the applied frequency,  $H_{res}$  is the magnetic field strength which resonates with the rf field and  $Mc^2$  is the rest energy of the ion. This equation indicates that the phase shift of the ion of which energy is  $E$  is equal to the area  $S$  in Fig. 27(a). In order to accelerate ions up to the desired energy, the phase shift must be less than  $180^\circ$  when the energy of the ions reaches the value of  $E_{res}$ . This condition is understood as follows. When the value of  $E_{res}$  is chosen so as to make the areas  $S_1$  and  $S_2$  the same, this condition implies that both  $S_1$  and  $S_2$  must be less than two.  $S_1$  and  $S_2$  are defined as are seen in Fig. 27 (b). The areas  $S_1$  and  $S_2$  are also functions of  $V_o$ , so that value of  $V_o$  which gives the following relation is the minimum rf voltage between the dees to accelerate the ions up to the desired energy.

$$|S_1| = |S_2| = 2.$$

The areas  $S_1$  and  $S_2$  were evaluated graphically by changing  $E_{res}$  for various values of  $V_o$ . The results of the calculations are shown in Fig. 28.

Furthermore, the initial phase of the ion is restricted by the conditions that the ion should not be defocused by electro-magnetic fields and should not hit the ion source after the first revolution. To find the latter condition, the electric field around the ion source was estimated by a model measurement. Then the ion paths of the first revolution were calculated by solving the equation of motion for the ion numerically. The results of this calculation are shown in Fig. 29.

Taking into account all the conditions, the minimum voltage above mentioned was estimated to be 80 kv. At the early stage of the initial testing of the cyclotron the efforts on obtaining ampler rf voltage across the dees was carried on without ion loading. The experimentally estimated minimum voltage, as is shown in Figs. 30 and 31, agrees well with the predicted value.

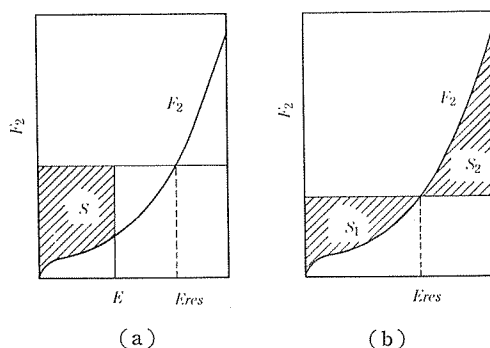


Fig. 27. Graphical illustration of the phase-shift calculation of the resonant ion.

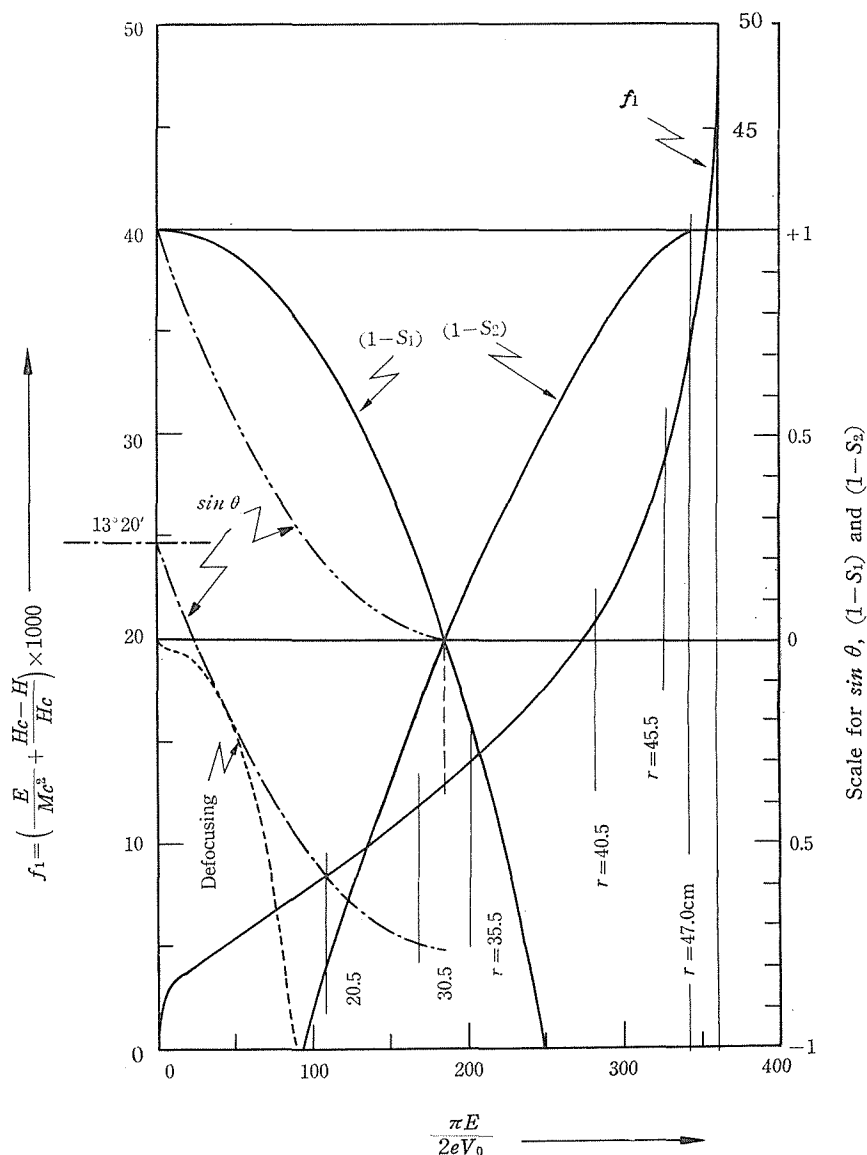


Fig. 28. Results on the phase-shift calculation of the ion. The curves in this figure are calculated with following condition;  $H_0=17,500$  gauss and  $V_0=140$  kv.

### B. Initial Testing and Troubles

The general assembling of the cyclotron had been finished by September, 1955, and then efforts in obtaining a sizable beam out of full radius had been carried on until January, 1956.

First of all, the oscillator system was adjusted by using two triodes TEN\* 167H's as test oscillator tubes. Without evacuating the dee chamber, the discharge

\* This tube is produced by Kobe Kogyo Corp.



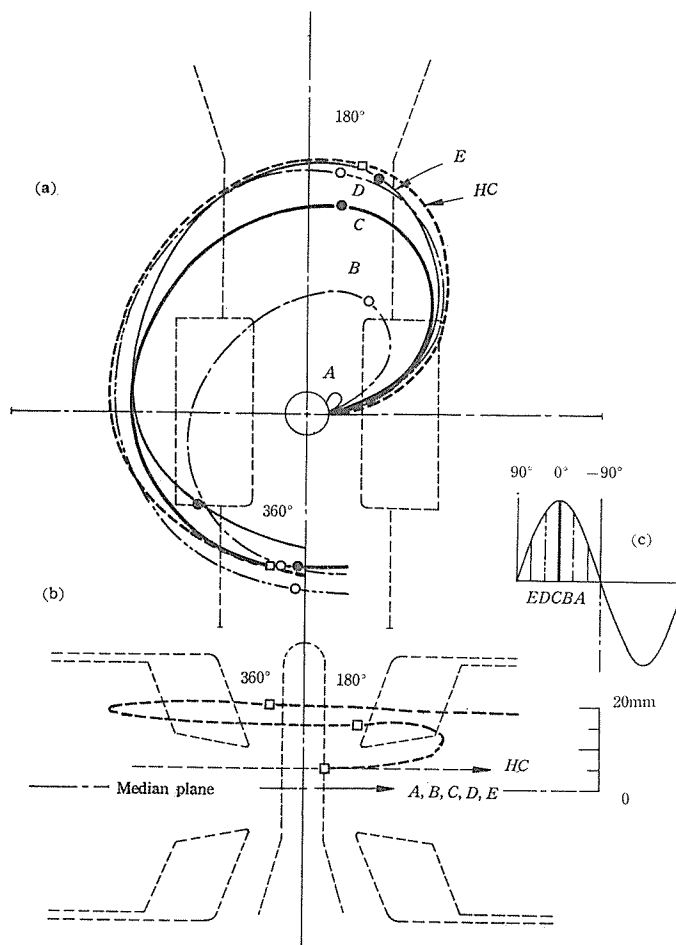


Fig. 29. Ion paths of the first revolution. The curves *A*, *B*, *C*, *D* and *E* in (a) show the paths of the ions which travel in the median plane and have started at the various phases with respect to the rf field as is shown in (c). The curve *HC* shows the horizontal projection of the path of the ion which has started in phase but at 5 mm higher level than the median plane. The vertical projection of *HC* is shown in (b). The circles and squares indicate the positions of the ions when the phase of the rf field reaches 180° or 360°.

between the dees was observed when the dee-to-dee voltage reached 20 kv, so that the mode of oscillation was assured to be push pull. No effect on this discharge was found by exciting the magnet up to 18 kilogauss. Then, the oscillator tubes were replaced by two RCA 5671 tubes. Evacuating the dee chamber, the dee-to-dee voltage reached 83 kv on October 31, 1955. This value of the dee-to-dee voltage corresponds to the minimum dee-to-dee voltage described in the previous section, 5-A. At this stage, the glow discharge from the plate coupling loop was observed and it broke the insulator of this coupling loop. Therefore, the same bias voltage

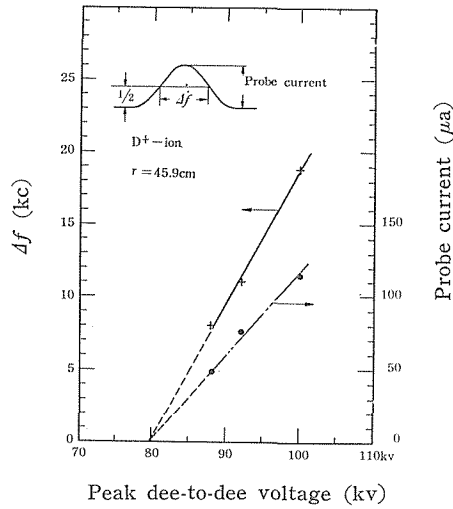


Fig. 30. Probe current at the radius of 45.9 cm versus the dee-to-dee rf voltage. The cross indicates the range of the oscillator frequency,  $\Delta f$ , where the probe current decreases to a half of the maximum.

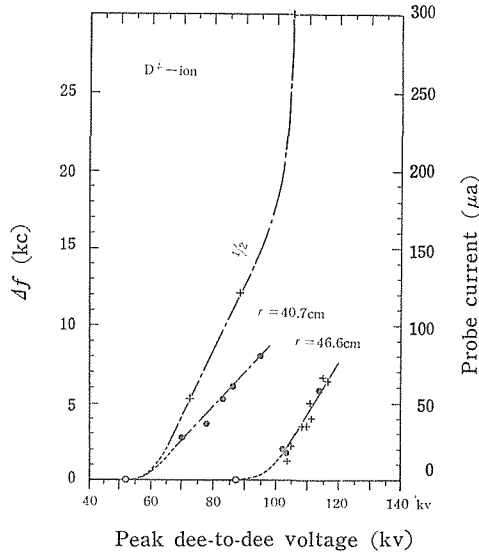


Fig. 31. Probe current at the radii of 40.7 cm and 46.6 cm.  
 Open circle : measured by a quartz probe, in Jan., 1956,  
 Solid circle : measured by a copper probe, in Feb., 1956,  
 Cross : measured by a copper probe, in July, 1956.

as the dee bias was applied to the loop, but no effect on ceasing this glow discharge was found. This trouble was overcome by changing the length of the transmission lines and the diameter of the guard electrode of the insulator.

At the early time, the ion beam was detected by a small strip of quartz or tantalum mounted on the probe which can be inserted between the dees along the center line. On October 31, 1955, the hydrogen molecular ions were loaded for

the first time, and observations on quartz probe showed that there was a sufficient beam at a radius of 30 cm to heat the probe red hot. By the middle of December, 1955, after six weeks of intermittent operation for adjusting the ion source, a deflected beam of  $2 \mu\text{a}$  had been obtained with the dee-to-dee voltage of 87 kv.

In order to measure the path of deflected beams, a number of 1 mm in diameter quartz rods were placed along the expected beam path. The deflected beam was strong enough to melt these quartz rods, and made it possible to estimate the beam direction. This method had been modified and used to measure the accurate beam path successfully.<sup>26)</sup> These measurements indicated that the angle of the joining duct to the beam focusing system had to be changed. The deflected beam of about  $20 \mu\text{a}$  had been obtained by February, 1956, with the dee-to-dee voltage of 114 kv. During the initial testing period the oscillation frequency and the dee-to-dee voltage became quite unstable about 10 minutes after the oscillator was fired, and also some troubles were found in the resonant circuit. These difficulties and their improvements will be discussed in the following section.

As was mentioned before, the resonant ion beam was accelerated up to full radius within a short period without serious troubles. This might be due to judicious alignment of the dees. Besides this, the oscillator system used — in particular, the dee-bias system — made rf oscillation stable against discharges inside the vacuum envelope, and it shortened the time to be spent for degassing of the vacuum envelope.

Some of the results obtained on the resonant ion beam are shown in Figs. 30, 31 and 32.

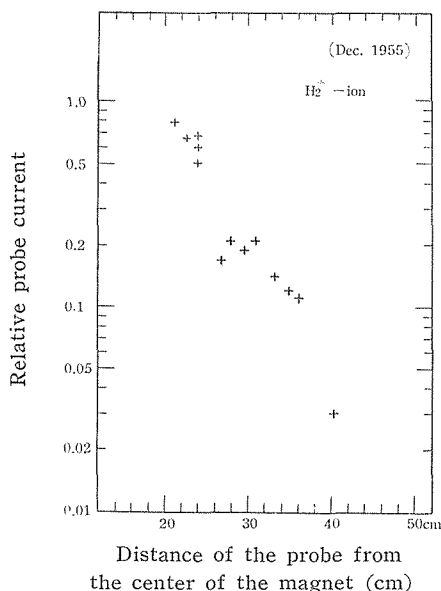


Fig. 32. Probe current with the peak dee-to-dee voltage of 41 kv. (Radial dependence of the resonant ion current.)

**C. Some Improvements**

After the initial test was performed successfully, the construction inside the building had been made during the next four years. The shielding of the cyclotron, the experimental room, the control room, the counting room and so on were constructed. During this period the intermittent testing and improvements on the cyclotron performance had been carried on.

First of all, the most weak point for continuous operation of the cyclotron was found to be the short-circuiting capacitor in the dee-stem-tanks and its contact mechanism. Non-copper parts used to construct the capacitor, such as aluminum plates, steel pins, brass washers and nuts and so on, were heated by the rf field. Consequently, zinc in brass was sputtered on the surface of insulators of the capacitor and other parts, and the contact mechanism became very loose by the rf heating after a few hour operation with the dee-to-dee voltage of 110 kv. These troubles are improved very much by plating copper on the brass parts. However, at the end of this period, the short-circuiting capacitor on the "north" side was dead shorted by deformation due to the excessive rf heating.

Since the constructions inside the building had been performed, further testing and efforts were carried on to make the cyclotron operation steady. Initially, the insulators of the termination capacitors were made of glass-bonded micas. These

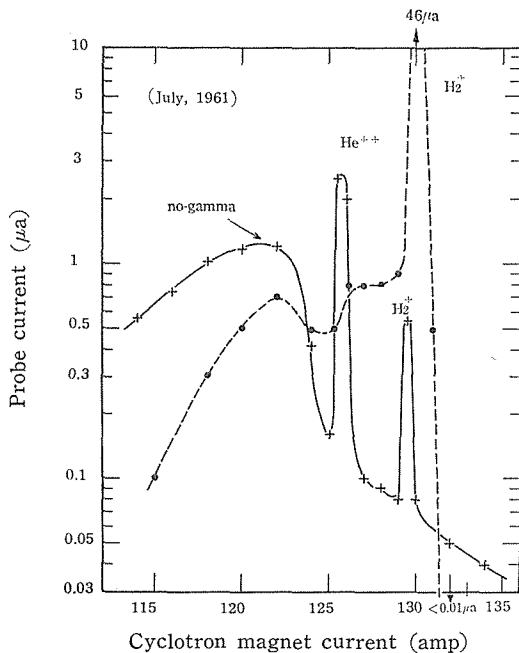


Fig. 33. Probe current versus the magnet current. The probe current was measured at the radius of 55.2 cm, so that this probe current represents the total deflected beam intensity.

insulators were replaced by those made of BeO which has excellent thermal conductivity compared with that of glass-bonded micas.

As was mentioned in the previous section, the oscillation frequency shifted considerably within a short period. Furthermore, a number of light points, called "lamps", were occasionally observed on the feelers when the oscillator was on. These lamps caused discharges around the ion source frequently. Extensive efforts were spent to remove these difficulties. Finally, by decreasing the rf dee voltage on the "north" dee, the frequency became considerably constant for many hours. At the same time, the number of "lamps" was decreased noticeably.

Alpha particles were also accelerated in this period, and characteristics of the alpha beam are shown in Fig. 33. The performances which were achieved by March, 1961, are listed in Table 1.

## 6. BEAM FOCUSING SYSTEM AND SCATTERING CHAMBER

The deflected beam is brought out through a duct made of brass without a magnetic shielding channel which might cause a serious asymmetry of the cyclotron magnetic field. It is very difficult to estimate the source point of this deflected beam beforehand, and the horizontal and vertical source points should be different each other and might vary with the conditions of the cyclotron operation. Therefore, in order to focus the deflected beam to the desired position in the experimental room, a pair of quadrupole magnets is employed. The use of a pair of quadrupole magnets has the following advantages when it is compared with that of a sector magnet: (1) Horizontal and vertical focal lengths can be changed separately, only by adjusting excitation current of each magnet. (2) By varying the focal lengths, the beam direction does not change. (3) A quite short focal length can be obtained, so that the magnets can be set close to the cyclotron.

Each quadrupole magnet used to focus the deflected beam has a rather large aperture of which radius is 12 cm, and its length is 25 cm. The profile of poles is an exact hyperbola, so that the magnetic field gradient,  $dB/dX$ , is constant within 0.5% over the whole aperture. The maximum field gradient is about 500 gauss/cm. This pair of quadrupole magnets is placed close to the cyclotron, and then it focuses the deflected beam on the center of the scattering chamber in the adjacent experimental room. The focused beam spot was observed by the aid of a television set, and its horizontal and vertical spreads at the optimum condition are about 7 and 9 mm, respectively.

The shielding wall between the cyclotron and experimental rooms is made of 160 cm thick ordinary concrete. In the middle of this wall, a rather wide tunnel is provided for carrying the equipments into the cyclotron room, when it is necessary. Usually, this tunnel is blocked up by a large water tank which is movable and shields the experimental room. The beam focused by the quadrupole magnets is led into the experimental room through a narrow channel in this water tank.

The scattering chamber of which inner radius is 51.8 cm is designed to use both nuclear plates or scintillation counters as detectors. A multiplate camera which can be mounted inside the chamber was constructed, and it consists of a multiplate-holder and a slit system. For the use of scintillation counters, a

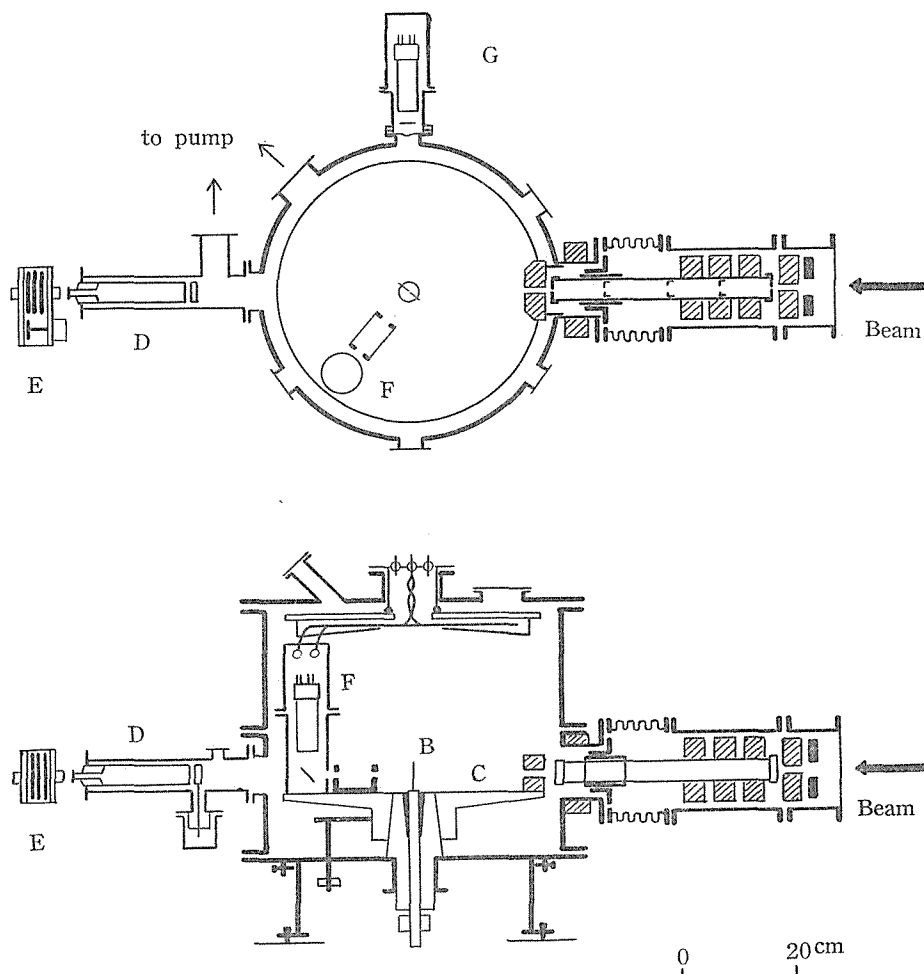


Fig. 34. Plan and elevation drawings of the scattering chamber.  
 A. Collimator, B. Target holder, C. Turntable, D. Faraday cup,  
 E. Apparatus for energy measurement, F. Detector, G. Monitor.

precision turntable is built into the scattering chamber and a scintillation counter can be set on it. The angular position of this turntable is reproducible within 0.05 degrees. The beam collimator is attached in front of the scattering chamber and it consists of two defining slits 36 cm apart and four anti-scattering slits. The defining slits are made of tantalum while the anti-scattering slits are made of aluminum. Three sets of defining slits having diameters of 1 mm, 2 mm and 3 mm are provided, and these slits can be changed easily. An additional slit having a diameter of 10 mm is placed in right front of the first defining slit and it is cooled by water. This additional slit protects the defining slit from ion bombardment of un-focused beams. The target can be supported on a pivot at the center of the scattering chamber, and the turntable and the pivot can turn separately. A gas target system also is provided. The beam passing through the

scattering chamber is collected by a Faraday cup which is 31 cm in inner diameter and 19.5 cm long. In front of the Faraday cup, an electro-magnet and a guard ring are provided to suppress the effects of secondary electrons. The details of the scattering chamber is described elsewhere.<sup>9)</sup> Plan and elevation drawings of the scattering chamber are shown in Fig. 34.

## 7. ACKNOWLEDGEMENTS

Throughout the design and reconstruction of the cyclotron, we have benefited by the help and advice of a number of the physicists as well as the technicians. First of all, we are deeply indebted to the late Professor Ernest O. Lawrence of the University of California who had kindly sent us the useful informations on the Crocker 60-inch cyclotron and also had made the arrangement for us to get informations from other institutes in the United States, to Dr. Hugo Atterling of Nobelinstitutet för Fysik in Stockholm who had sent us the valuable informations on the "short-circuiting" condenser, to Professor M. Stanley Livingston of MIT who had sent us the blue prints of the MIT cyclotron, to Professor Donald W. Kerst who had offered the useful knowledge on the oscillator system of the cyclotron in the University of Illinois, to Prof. Seishi Kikuchi of the Osaka University\* who had introduced us the valuable articles on designing and practices of cyclotrons, and to Dr. Harry C. Kelly of National Science Foundation, Washington D. C., who made RCA oscillator tubes available for us.

Appreciations are also due to Drs. Toshio Azuma, Masakatsu Sakisaka, Yoshio Saji, Jiro Muto, Tomonori Hyodo, Asao Kusumegi, Hisashi Yamaguchi, Muneo Takai and Kunihiro Tsumori, Messrs. Sanao Okamoto, Hidehiko Ito, Kiyoji Fukunaga, Kyoji Harada, Kenji Takumi, C. L. Wang and Hideo Aisu for their technical assistance during the construction and the testing of the cyclotron.

Thanks are also due to Yahata Iron and Steel Co., Ltd., Sumitomo Metal Industries Ltd., Mitsubishi Electric Mfg. Co., Ltd., Kobe Kogyo Corporation and Kobe Steel Works, Ltd. for their efforts in constructing the main parts of the cyclotron.

The reconstruction of this cyclotron was made possible by financial supports from a number of companies and the interested people beside the budget allowed by the Ministry of Education. Kyoto City kindly offered the use of the building which was used as a hydroelectric power plant in the past, and Kansai Electric Power Co., Ltd. also offered the electric equipments of power supply for our cyclotron.

We also wish to express our appreciation to the former Presidents, Professors Risaburo Torigai and Shunjiro Hattori, the late former Director of our Institute Professor Senji Uchino, the former Directors, Professors Masao Horio, Sankichi Takei and Risaburo Nakai for their encouragement and support throughout this project. The help of the staff in the administration office of the Kyoto University and of our Institute are greatly acknowledged.

Finally, it is our great pleasure to report this paper to our respected leader,

---

\* Now, Director General of Japan Atomic Energy Research Institute, Tokai-mura, Ibaraki-ken.

Professor Bunsaku Arakatsu who has kept his warm eye on our efforts in the reconstruction and congratulated our successful accomplishment of this project.

#### REFERENCES

- (1) M. S. Livingston, *J. Appl. Phys.*, **15**, 2 (1944) and **15**, 128 (1944).
- (2) H. Atterling, *Arkiv Fysik*, **2**, 559 (1949).
- (3) H. L. Anderson and J. Marshall, The University of Chicago 170-inch Synchrocyclotron Progress Report I July 1947-July 1948, II July 1948-July 1949 and III July 1949-July 1950.
- (4) J. W. Gallop, Notes on a tour of American fixed frequency cyclotrons in the autumn of 1950. Medical Research Council, Hammersmith Hospital, London.
- (5) K. Kimura, Y. Uemura, R. Ishiwari, J. Kokame, K. Fukunaga, A. Katase, J. Muto, I. Kumabe, H. Ogata, T. Ohama and Y. Ohmori, *J. Phys. Soc. Japan.*, **17**, 6 (1962).
- (6) R. Ishiwari, This Bulletin, **39**, 287 (1961).
- (7) J. Kokame, *J. Phys. Soc. Japan.*, **16**, 2101 (1961).
- (8) T. Yanabu, *J. Phys. Soc. Japan.*, **16**, 2118 (1961).
- (9) T. Yanabu, S. Yamashita, T. Nakamura, K. Takamatsu, A. Masaike, S. Kakigi, D. C. Nguyen and K. Takimoto, *J. Phys. Soc. Japan.*, **16**, 2594 (1961).
- (10) S. Yamashita, *J. Phys. Soc. Japan.*, **16**, 2378 (1961).
- (11) T. Nakamura, K. Takamatsu, A. Masaike, S. Kakigi, D. C. Nguyen, S. Yamashita and T. Yanabu, *J. Phys. Soc. Japan.*, **17**, 19 (1961).
- (12) K. Miyake, This Bulletin, **39**, 313 (1961).
- (13) M. E. Rose, *Phys. Rev.*, **53**, 715 (1938).
- (14) W. E. Danforth, *Rev. Sci. Instr.*, **10**, 211 (1939).
- (15) K. R. MacKenzie, *Rev. Sci. Instr.*, **22**, 302 (1951).
- (16) F. H. Schmidt, G. E. Farwell, J. E. Henderson, T. J. Morgan and J. F. Streib, *Rev. Sci. Instr.*, **25**, 499 (1954).
- (17) J. Backus, *Rev. Sci. Instr.*, **22**, 84 (1951).
- (18) S. Shimizu, A. Katase, H. Takekoshi, K. Takumi and E. Takekoshi, This Bulletin, **32**, 214 (1954).
- (19) H. Attering and G. Lindström, *Arkiv Fysik*, **15**, 483 (1959).
- (20) F. H. Schmidt and M. J. Jakobson, *Rev. Sci. Instr.*, **25**, 136 (1954).
- (21) M. S. Livingston, *Rev. Modern Phys.*, **18**, 293 (1946).
- (22) E. C. Crittenden Jr. and W. E. Parkins, *J. Appl. Phys.*, **17**, 444 (1946).
- (23) P. G. Kruger, G. K. Groetzinger, J. R. Richardson, E. M. Lyman, W. E. Nelson, G. Schwarz, J. B. Greene, N. C. Colby, R. W. Lee, C. E. McClellan, D. Scag, L. Smith and F. K. Tallmadge, *Rev. Sci. Instr.*, **15**, 333 (1944).
- (24) M. E. Rose, *Phys. Rev.*, **53**, 392 (1938).
- (25) B. L. Cohen, *Rev. Sci. Instr.*, **24**, 589 (1953).
- (26) K. Kimura, J. Kokame and S. Yamashita, *Rev. Sci. Instr.*, **29**, 142 (1958).